Winter 1995

Compensation and Characterization of Gallium Arsenide

Randy A. Roush
Old Dominion University

COMPENSATION AND CHARACTERIZATION OF GALLIUM ARSENIDE

by Randy A. Roush
B.S.E.E. May, 1989, Old Dominion University
M.S.E.E. December, 1990, Old Dominion University

A Dissertation Submitted to the Faculty of
Old Dominion University in Partial Fulfillment of the
Requirements for the Degree of

DOCTOR OF PHILOSOPHY

ELECTRICAL ENGINEERING

OLD DOMINION UNIVERSITY
December, 1995

Approved by:

_____

K. H. Schoenbach (Director)

_____

_____

_____

ABSTRACT

The properties of transition metals in gallium arsenide have been previously investigated extensively with respect to activation energies, but little effort has been made to correlate processing parameters with electronic characteristics. Diffusion of copper in gallium arsenide is of technological importance due to the development of GaAs:Cu bistable photoconductive devices. Several techniques are demonstrated in this work to develop and characterize compensated gallium arsenide wafers. The material is created by the thermal diffusion of copper into silicon-doped GaAs. Transition metals generally form deep and shallow acceptors in GaAs, and therefore compensation is possible by material processing such that the shallow silicon donors are compensated by deep acceptors. Copper is an example of a transition metal that forms deep acceptors in GaAs, and therefore this work will focus on the compensation and characterization of GaAs:Si:Cu.

The compensation of the material has shown that the lower diffusion temperatures (500-600 °C) form primarily the well-known Cu_B centers whereas the higher temperature anneals (>750 °C) result in the formation of Cu_A. Using *compensation curves,* the copper density is found by comparing the compensation temperature with copper solubility curves given by others. These curves also show that the formation of Cu_B , EL2, and Cu_A can be manipulated by varying processing parameters such as annealing temperature and arsenic pressure. The compensation results are confirmed using Temperature-Dependent Hall

(TDH) measurements to detect the copper levels. Also, the photoconductive properties of the material under illumination from 1.06 and 2.1 μm wavelength laser pulses have been used to demonstrate the effects of the different processing procedures. The persistent photoconductivity inherent to these devices under illumination from the 1.06 μm laser pulse is used to predict the concentration of the Cu_B level, and the fast hole capture times of the various acceptors are found through the response to a 140 ps (FWHM), 2.1 μm laser pulse. Finally, the physical distribution of the copper atoms in the gallium arsenide wafer is examined using Glow Discharge and Secondary Ion Mass Spectroscopy (GDMS and SIMS). These techniques have been used to show that the copper diffusion in gallium arsenide is non-uniform with respect to depth and surface position.

TABLE OF CONTENTS

LIST OF FIGURES

CHAPTER 1

INTRODUCTION

The preparation of gallium arsenide has been extensively studied for uses in light emission devices such as LED's and lasers. Since GaAs is a direct-band semiconductor, the light emission properties are far more efficient than those of indirect-band materials such as silicon. The reason for this advantage is that phonon interaction is not required in order for a carrier in the upper band to transition to the lower band. Another use for gallium arsenide involves the photoconductive properties. Compared to other semiconductor materials, GaAs has several advantages as a photoconductor. First, the bandgap is large enough to hold off relatively high electric fields but low enough to allow band-band photo-excitation using near-IR lasers. Many of the electronic and photoconductive properties of gallium arsenide have been explored for semi-insulating material and junction devices. The market for these materials is quite extensive, and support for research is growing. The use of gallium arsenide doped with transition metals such as copper for photoconductive devices may also show enough promise to establish a market in the device community. It is the purpose of this work to explore the behavior of copper in gallium arsenide with respect to the material preparation, photoconductive properties, and electronic characteristics. The idea is to provide new information with regard to transition metal dopants in gallium arsenide.

Gallium arsenide is prepared by manufacturers in many ways. Typically, bulk GaAs is either pulled from a melt (LEC- Liquid-Encapsulated Czochralski) or boat-grown (HB- Horizontal Bridgeman). Figure 1.1 shows a comparison between the two methods.[1] Typically, the HB method is used to produce n-type, silicon-doped GaAs because the tube system is made from SiO_2 which inevitably donates some silicon. The arsenic source in the quartz tube is important in maintaining an arsenic over-pressure such that the GaAs molar fraction is maintained. The fact that GaAs is a compound semiconductor means that during such growth there will be intrinsic defect formation. For example, perfect control of the arsenic over-pressure is needed to maintain the proper mol-fraction, but the cooling of the melt will still result in some mis-placed arsenic and gallium atoms. This will introduce vacancy and substitutional defects in the crystal lattice.

Also, there will be impurities in the melt that give rise to additional energy levels in the bandgap. Carbon is a common impurity in gallium arsenide which seems be present for several different growth techniques. Intentional introduction of specific impurities into the melt provides a means of doping that is desirable in terms of uniformity and ability to control the doping concentration. In the case of copper doping, a melt system must be dedicated to only copper due to contamination for other uses. Therefore, copper doping by introduction in the melt will only be achieved when there is adequate interest in the material to assemble a growth system strictly dedicated to the production of copper-doped gallium arsenide.

Copper-doped gallium arsenide is potentially a technologically important semiconductor as it has been used as a photoconductive switch operating on a nanosecond

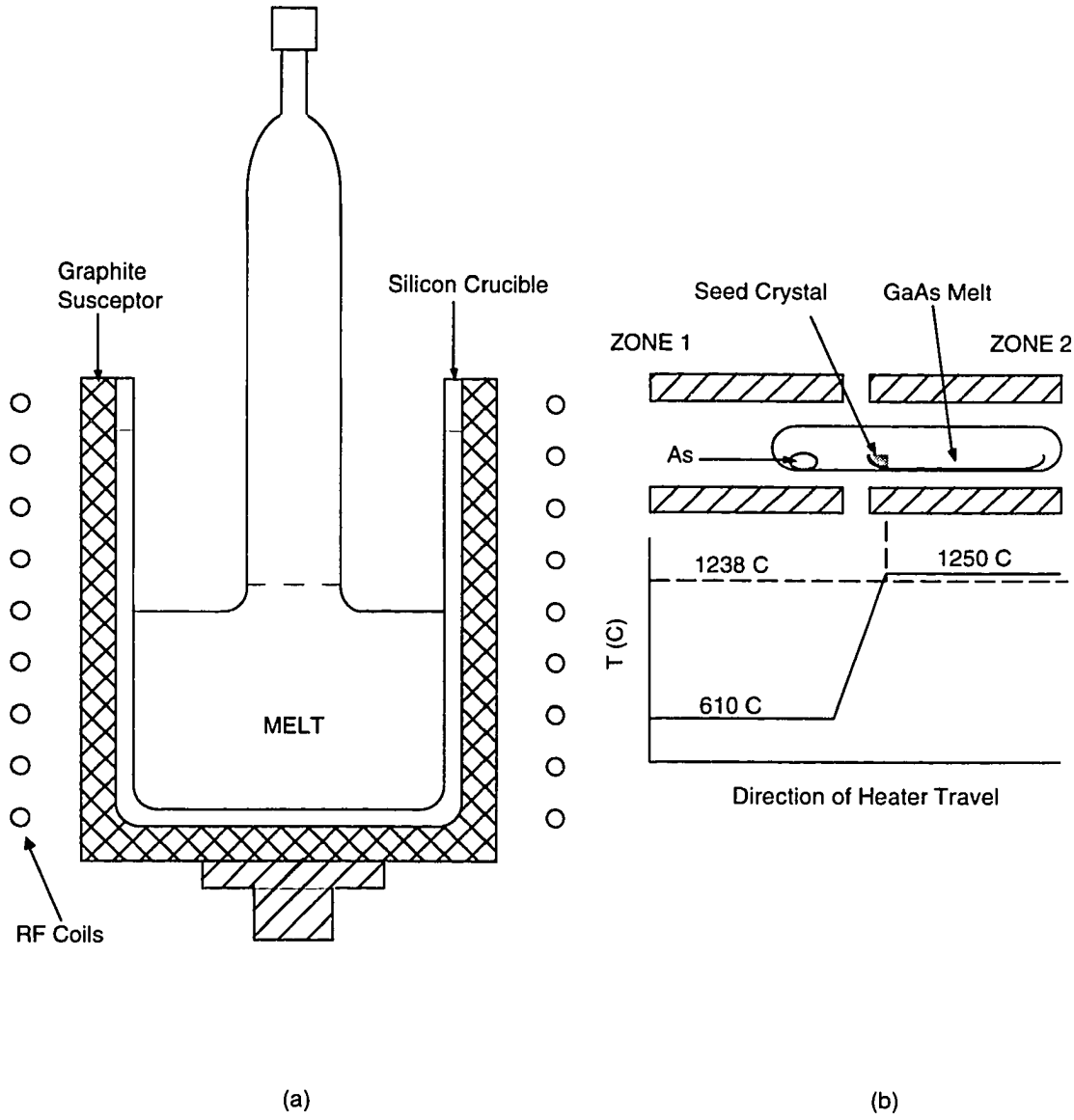

Figure 1.1. (a)Czochralski and (b) Bridgeman techniques for gallium arsenide growth.

time scale.[2,3,4] This material has been produced by electrically compensating n-type, silicon-doped gallium arsenide through a thermal copper-diffusion process. Typically, the Si-doped GaAs is placed in a diffusion furnace along with a solid source of copper at a set temperature and for a given time.[5] The resulting material has energy levels that consist of deep copper acceptors and shallow silicon donors. The ratio of the concentrations of the densities of these centers determines the compensation. It is desired that the material is highly resistive in order that a voltage may be applied and photoconductive properties explored.

The Bistable Optically controlled Semiconductor Switch (BOSS) is *turned on* by pulsed, infrared excitation (1.06 μm wavelength laser pulse) of electrons trapped at the deep copper acceptor known as Cu_B (see figure 1.2).[3] The *on-state* is sustained by slow electron capture at Cu_B resulting in a large electron population in the conduction band that remains for several microseconds after the laser pulse ends. Infrared quenching of this on-state photocurrent is accomplished using a 2.1 μm wavelength laser pulse to stimulate fast, band-band recombination.[4] This *turn*-off laser pulse causes residual holes left in Cu_B during the on-state to be excited into the valence band, and thus band-band recombination returns the semiconductor to the *off-state*. The BOSS material (GaAs:Si:Cu) is highly resistive in the natural off-state, and there must be a process by which it is produced repeatably and consistently. This means that the technique of compensation must be addressed first. The compensation process involves the thermal diffusion of copper into silicon-doped gallium arsenide. In chapters two and three, the compensation of gallium arsenide using thermal techniques will be carefully addressed. The goal is to provide a

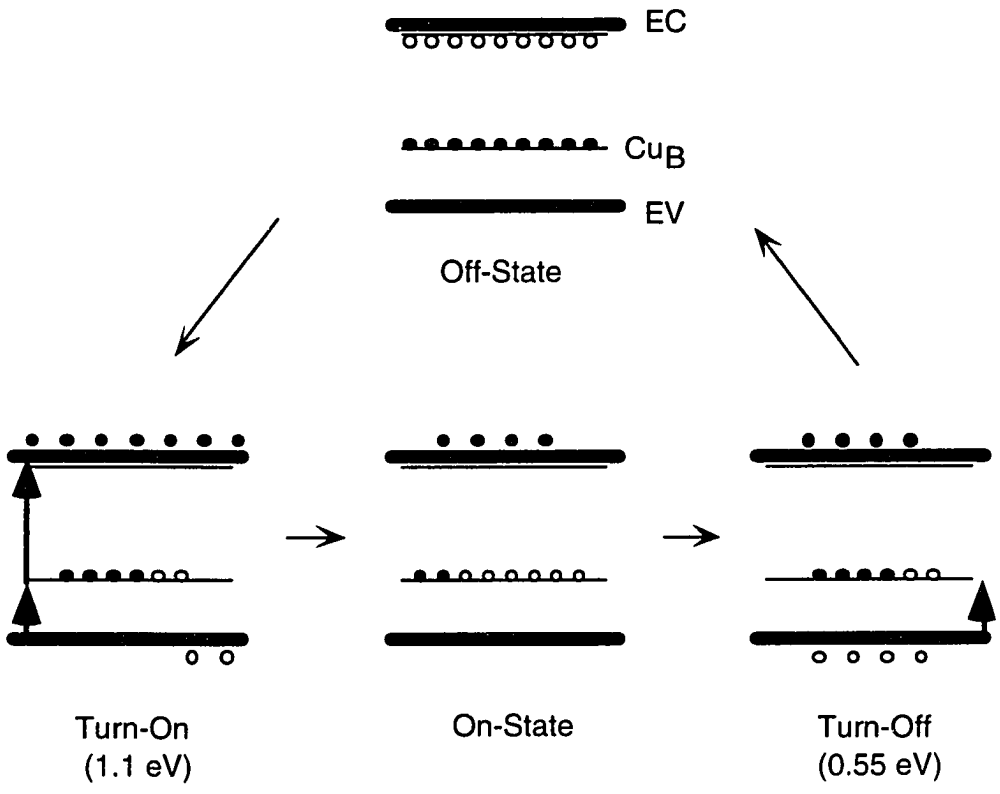

Figure 1.2. BOSS switching cycle band-diagrams.

compensated semiconductor suitable for testing in a switching environment. Not only will the compensated material be examined, but the uncompensated material shall be addressed with equal interest. The reason for this approach is the understanding that the process by which the compensation is achieved provides the desired information. After each sample is thermally treated, a series of characterization experiments are done in order to define the material properties with respect to the processing conditions.

The characterization experiments are designed to determine the extent of compensation, and to detect the deep centers that have been introduced into the crystal. The characterization techniques that will be discussed in later chapters are designed to provide feedback to the device fabrication. First, the Hall effect is used in order to determine if the material is n or p-type. This is important because when doping an n-type material with acceptors, a knowledge of the post-diffusion carrier type tells if the acceptor density has exceeded the donor density. Also, the conductivity and carrier density are measured which allows the compensation to be defined.

Next, the material must be characterized to find the nature of the deep centers that have been formed. This involves the use of Temperature-Dependent Hall effect spectroscopy (TDH)[6]. The TDH measurements are designed to use the hole-density vs temperature data to identify deep levels in the samples. The purpose of these measurements is to provide needed information to the modeling and processing efforts. Specifically, it is of interest to determine the changes in the copper levels arising from an increase in doping density (ie. diffusion temperature).

The bistable switching characteristics of this material also provide needed deep level information. The excitation of the device using a 1.06 μm wavelength laser source (see figure 1.2) excites photoconductivity that saturates with laser intensity in such a way that the relative deep center densities can be obtained. A fast (100 ps) laser source can be used to excite the switch such that the hole trapping times can be obtained as functions of the doping density. All of this information is important to the operation of the BOSS bistable switch, and must be obtained in order to further develop this technology.

Equally important as electronic characterization is the physical characterization of the crystal. In order to determine the spatial inhomogeneities associated with the copper diffusion process, two techniques are to be employed: Glow Discharge Mass Spectroscopy (GDMS) and Secondary Ion Mass Spectroscopy (SIMS).[7] The GDMS system is designed to sputter material from the surface in a spot which can be analyzed to determine the constituents. This technique is used for depth profiling because the sputter rate is relatively high and therefore the entire depth of the material can be characterized in a reasonable amount of time. The SIMS technique is similar in that a sputtering technique is used. A portion of the sputtered atoms are ions (called secondary ions) which are analyzed through the mass spectrometer. This system is most suited for shallow depths, and therefore it is useful in surface profiling. These two techniques (SIMS and GDMS) will allow a complete physical picture of the copper diffusion in GaAs to be observed.

In the following chapters, the compensation and characterization of copper diffused GaAs will be closely examined. The compensation will be defined with an analytical model which will be matched to the experimental data under several different

processing conditions. Also the effects of heat treatment will be noted with respect to the compensation process. The samples used in the compensation experiments will also be analyzed in order to determine the nature of the copper impurities in GaAs. This will involve the characterization techniques outlined above. The goal of this research is to provide needed information to switching technologies that require bistable optically controlled devices, and to provide general insight into the nature of the diffusion of transition metals in semiconductors.

CHAPTER 2

MODELING

Several analytical and numerical models of photoconductive semiconductor switches have been introduced over the last decade. In this section, a set of equations based on drift/diffusion in copper-doped gallium arsenide will be shown, and this system of equations has been solved numerically by Brinkmann.[8] The numerical results will be used to show the success of the numerical calculations in predicting the BOSS effect described in the previous chapter. Also, an analytical approach will be developed to show the effects that are to be experimentally exploited in this work. Specifically, it is of interest to determine the maximum steady on-state conductivity generated using the turn-on laser pulse, and to measure the hole re-capture times for excitation with the turn-off laser. Each of these effects are to be investigated for several different doping densities, and the results will be compared to those of the numerical model to determine consistency. In order to demonstrate the effects on the sample dark-conductivity of changing the doping densities, an analytical model will be developed for the electrical compensation process. This is important because the base material from which all of the results in this work must come is developed through the compensation process.

2.1 Drift-Diffusion

The drift-diffusion model involves a few assumptions which allow us to use some known distribution functions and simplify the Boltzmann equation into the set of equations to be solved. Electrons and holes (negative and positive charges) will drift under the influence of an electric field and diffuse due to concentration gradients. The drift-diffusion equations are written as,[9]

$$\frac{\partial n}{\partial t} + \nabla \cdot (-v_n(E)n - D_n(E)\nabla n) = \dot{n} \qquad 2.1$$

$$\frac{\partial p}{\partial t} + \nabla \cdot (v_p(E)p - D_p(E)\nabla p) = \dot{p} \qquad 2.2$$

where v is the drift velocity, D is the diffusion coefficient, n is the electron concentration, and p is the hole concentration. The Poisson equation is also needed to relate the electric field to the charge density,

$$-\varepsilon_o \varepsilon_r \nabla^2 \phi = \rho \qquad 2.3$$

where ϕ is the electrical potential. Next, the deep levels in the semiconductor and trapping rates must be defined. The idea here is to define a set space in which the electron density, hole density, electrical potential, and occupation number can all be explicitly found.

2.2 Trapping/Emission Kinetics

Consider the band diagram shown in figure 2.2.1. Electrons and holes can be trapped by or emitted from the various levels. Therefore, at any time the electron occupation of each individual level can be defined using the electron occupation number designated as 'r_i' where the subscript is an index which represent a given energy level. The occupation number is defined as, $r_i = n_i/N_i$, where n_i is the electron concentration of

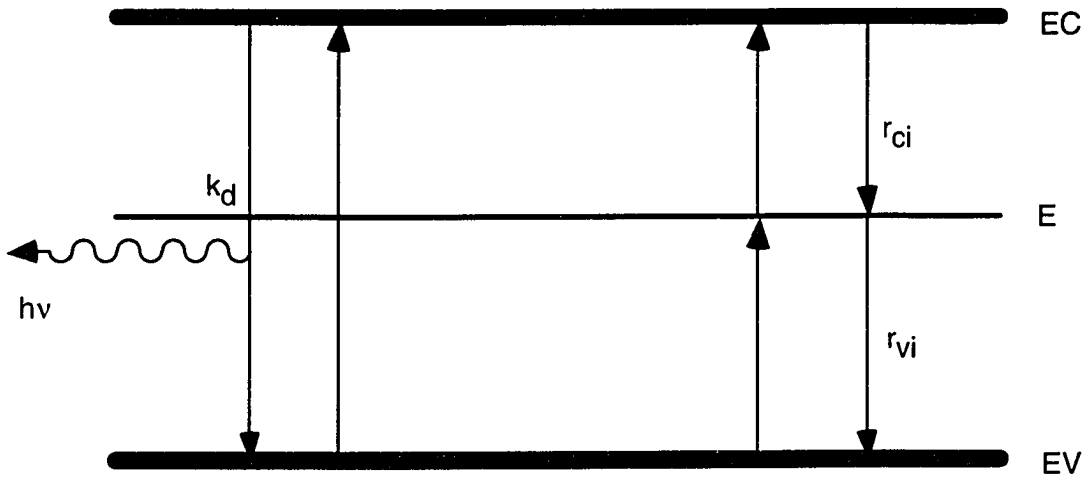

Figure 2.2.1. Band diagram showing trapping/recombination rates.

the deep center, and N_i is the total concentration of the level. The charge density can be written to include the free and fixed charge using the occupation numbers,

$$\rho = q(p - n - \sum N_i r_i) + \rho_{BG} \qquad 2.4$$

where ρ_{BG} represents the background charge. Next, the rates of change of the electron and hole concentrations are written in terms of conduction-valence band transitions ($\dot{n}_{cv}$), and the trapping terms,

$$\dot{n} = \dot{n}_{cv} + \sum_i N_i r_{ci} \qquad 2.5$$

$$\dot{p} = \dot{n}_{cv} + \sum_i N_i r_{vi} \qquad 2.6$$

$$\dot{r}_i = \dot{r}_{vi} - \dot{r}_{ci} \qquad 2.7$$

where $\dot{r}_{ci}$ and $\dot{r}_{vi}$ are described in figure 2.2.1. The rate of band-band transitions depends on the direct recombination coefficient (k_d) and the thermal emission term (e_{th}),

$$\dot{n}_{cv} = e_{th} - k_d np \qquad 2.8$$

The thermal emission term in 2.8 can be written in terms of the intrinsic carrier concentration, n_i, so that 2.8 becomes,

$$\dot{n}_{cv} = k_d(n_i^2 - np) \qquad 2.9$$

which describes the deviance of the carrier densities from equilibrium. The trapping of electrons follows the total trapping rate, $N_i \dot{r}_i$, which can be written in terms of a constant, the carrier density, and the number of empty traps ($k_{ci} N_i (1 - r_i) n$). Using these equations, the terms (see figure 2.2.1) can be written,

$$\dot{r}_{ci} = k_{ci}\left[\frac{r_{i,eq}}{1-r_{i,eq}} r_i n_{eq} - (1-r_i)n\right] \qquad 2.10$$

$$\dot{r}_{vi} = k_{vi}\left[\frac{r_{i,eq}}{1-r_{i,eq}} (1-r_i) p_{eq} - r_i p\right] \qquad 2.11$$

where k_{ci}, k_{vi} are directly proportional to the capture cross-sections with a proportionality constant that is effectively a trapping 'speed'.

2.3 System of Equations

A system of equations, based on the previous discussion was developed, and numerically solved by Brinkmann[8]. The energy levels involved in this system are shown in figure 2.3.1. Also, the effects of the two laser pulses are included to simulate the BOSS switching effect. Equation 2.9 is modified to include two-photon ionization,

$$\dot{n}_{cv} = k_d (n_i^2 - np) + \beta \frac{h\nu}{2} \Phi_{hi}^2 \qquad 2.12$$

where k_d is the direct recombination coefficient, β is the constant for two-photon processes, $h\nu$ is the photon energy (1.17 eV), n_i is the intrinsic carrier concentration, and Φ_{hi} is the short-wavelength laser photon flux. The terms describing the transitions to and from the deep levels contain the effects of stimulated emission due to the external laser irradiation. The transition terms can then be written following equations 2.10, 2.11,

$$\dot{r}_{ci} = k_{ci}\left[\frac{r_{i,eq}}{1-r_{i,eq}} r_i n_{eq} - (1-r_i)n\right] + \sigma_{ci}^{o}(h\nu_{lo})\Phi_{lo} + \sigma_{ci}^{o}(h\nu_{hi})\Phi_{hi} \qquad 2.13$$

$$\dot{r}_{vi} = k_{vi}\left[\frac{r_{i,eq}}{1-r_{i,eq}} (1-r_i) p_{eq} - r_i p\right] + \sigma_{vi}^{o}(h\nu_{lo})\Phi_{lo} + \sigma_{vi}^{o}(h\nu_{hi})\Phi_{hi} \qquad 2.14$$

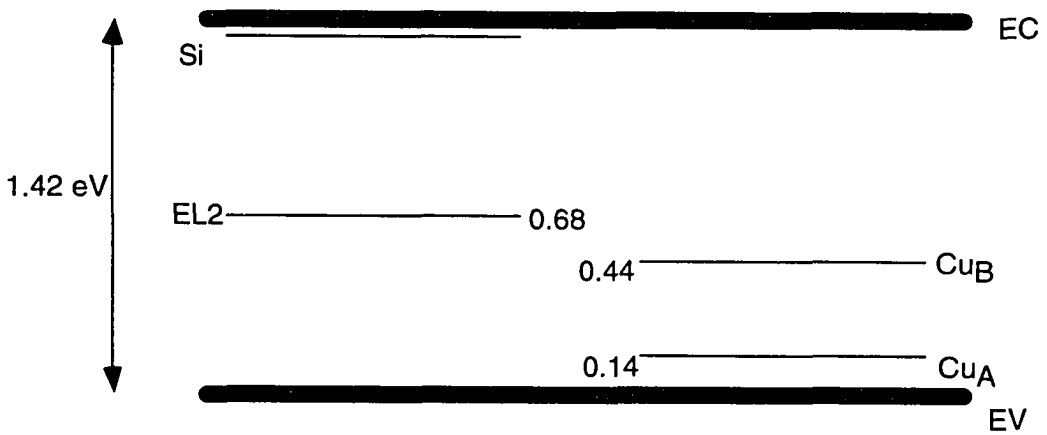

Figure 2.3.1. Band diagram for the BOSS model.

where the photo-ionization cross sections for electrons (σ_{ci}^{o}) and holes (σ_{vi}^{o}) in the i^{th} deep level are assumed to be independent of the photon energy. These zero for photon energies too small to induce a particular transition. The subscripts "hi" and "lo" represent the higher frequency (turn-on) and lower frequency (turn-off) laser pulses. The eq subscript is used to indicate the equilibrium values. Using two copper levels (Cu_A and Cu_B), the native EL2 level, and a recombination center, the curves shown in figure 2.3.2 are generated using this model.[8] This figure is in qualitative agreement with experimental curves that have been previously shown.[3,4] This simulation has been altered to include the effects of a third copper level (Cu_C), and again the experimental results were qualitatively matched. Also, the laser source functions were changed to match those involved in the experiments that are to be described in following sections. The purpose of this is to generate curves that match the conditions described in the next section concerning the IR-photoconductivity.

2.4 Infrared Photoconductivity

In later chapters, the two laser pulses used in the BOSS switching will be examined experimentally with respect to photoconductivity saturation by the turn-on pulse, and deep level detection using the turn-off pulse. Therefore it is instructive to further develop these ideas analytically. First, equations 2.5-2.7 can be written,

$$\dot{n} = G_n - U_n \qquad 2.15$$

$$\dot{p} = G_p - U_p \qquad 2.16$$

$$\dot{r}_i = \dot{r}_{ci} + \dot{r}_{vi} \qquad 2.17$$

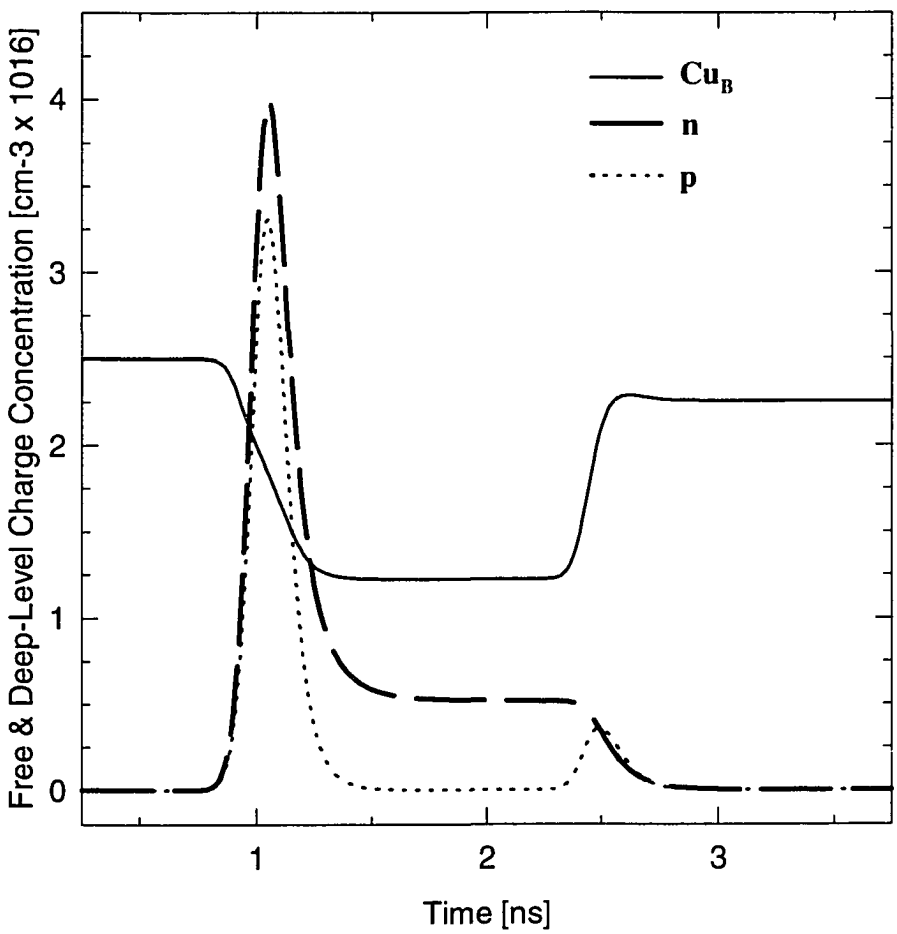

Figure 2.3.2. Switching model results, showing the rates of change of the charge trapped in Cu_B and the free carriers.

where G and U represent generation and recombination terms, and r_i is the occupation number defined as the ratio of trapped charge to total trap density as before (n_{Ti}/N_{Ti}). The recombination is expressed as,

$$U_n = k_d np + \sum_{i=1}^{m} c_{ni} n(N_{Ti} - n_{Ti}) \qquad 2.18$$

$$U_p = k_d np + \sum_{i=1}^{m} c_{pi} p n_{Ti} \qquad 2.19$$

where k_d is the direct recombination term (cm^3/s), c_n and c_p are the capture parameters (cm^3/s), and the subscript 'i' represents the various levels to be considered. The electrical conductivity can be written in terms of the free electron and hole concentrations (n,p),

$$\sigma = \mu_n nq + \mu_p pq \qquad 2.20$$

where μ is the mobility, and q is the electronic charge. Two special cases will be investigated here. The first will involve the excitation of electrons from Cu_B into the conduction band using the turn-on laser pulse (λ = 1.1 μm), and the second case is that of hole excitation from the various copper levels into the valence band using the turn-off laser (λ = 2.1 μm).[10]

For the case of irradiation with the 1.1 μm laser pulse, the maximum steady on-state conductivity is defined by assuming that the Cu_B level is approximately full of electrons initially, and that all of these electrons are excited into the conduction band by the laser pulse. These assumptions are justified by measurements of the Fermi level (obtained through Hall measurements) which has been located between the Cu_B level and the middle of the bandgap, and the fact that saturation of the photocurrent generated from

the photoexcitation of Cu_B must occur when the Cu_B level becomes filled with holes. A final consideration is that of hole excitation from Cu_B into the valence band which occurs during excitation by the 1.1 μm laser pulse. The cross section for electron photoexcitation (10^{-17} cm^2) is an order of magnitude smaller than that for holes (10^{-16} cm^2)[11], however, the combination of fast hole capture and slow electron capture processes at Cu_B causes the electron concentration at Cu_B to become depleted[2] after application of a 20 ns FWHM (1.1 μm) laser pulse. Direct (band-band) recombination is then the loss mechanism. Therefore, the maximum steady on-state conductivity (σ_{ss}) may be written as,

$$\sigma_{ss} = \mu_n N_{CuB} q \qquad 2.21$$

where N_{CuB} is the total density of the Cu_B level.[10] It should be noted that the photon energy of the turn-on laser is sufficient to excite electrons from Cu_B into the conduction band while excluding transitions from Cu_A and Cu_C into the conduction band.

Next, the second case of hole excitation from the copper levels into the valence band using the 2 μm laser pulse will be explored. This consideration is important because, for the BOSS device operation, the electron current generated by the turn-on laser is quenched by direct recombination with holes generated by the turn-off laser (2 μm). Therefore, the hole capture cannot be too fast or there will be negligible quenching effect. Also, investigating the hole capture processes gives insight into the deep level structure in the switch material. The hole capture time constant may be determined by irradiating the switch with the 2 μm laser pulse, and measuring the generated photocurrent decay during the time after the peak laser intensity. For this case, the electron current is small compared to hole density thus equations 2.15 and 2.18 are eliminated, because the 2 μm

wavelength has a corresponding photon energy that excludes transitions from any known copper acceptor into the conduction band. Assuming that three copper levels are present, the conductivity of the switch after the laser pulse has ended involves a generation term (G_p) in which emission must be considered,

$$G_p = \sum_{i=1}^{3} e_{pi} N_{Ti} (1 - r_i) \qquad 2.22$$

where e_{pi} is the emission parameter for each level (s^{-1}), and r_i is defined as before (n_{Ti}/N_{Ti}). Since the electron current has been neglected, then the direct recombination term in 2.19 can also be neglected. Rewriting 2.16 to include 2.19 and 2.22, and linearizing ($r_i p \approx p$) gives,

$$\frac{dp}{dt} = p(-c_{p1} N_{CuA} - c_{p2} N_{CuB} - c_{p3} N_{CuC}) + (1 - r_1) e_{p1} N_{CuA} + (1 - r_2) e_{p2} N_{CuB} + (1 - r_3) e_{p3} N_{CuC} \qquad 2.23$$

where $r_1 = n_{CuA}/N_{CuA}$, $r_2 = n_{CuB}/N_{CuB}$, and $r_3 = n_{CuC}/N_{CuC}$ are the occupation numbers for the deep acceptor levels. The occupation numbers may be written following 2.17 as,

$$\frac{dr_1}{dt} = e_{p1}(1 - r_1) - c_{p1} p \qquad 2.24$$

$$\frac{dr_2}{dt} = e_{p2}(1 - r_2) - c_{p2} p \qquad 2.25$$

$$\frac{dr_3}{dt} = e_{p3}(1 - r_3) - c_{p3} p \qquad 2.26$$

Now, in order to simplify the analytical solution, state variables are defined. This is done by setting $1-r_i \equiv x_i$, and therefore $dx/dr = -1$. This leads to the set of equations involving four state-variables, p, x_1, x_2, and x_3,

$$\frac{dp}{dt} = pC_p + e_{p1}N_1x_1 + e_{p2}N_2x_2 + e_{p3}N_3x_3 \qquad 2.27$$

where $C_p = -c_{p1}N_1 - c_{p2}N_2 - c_{p3}N_3$, and,

$$\frac{dx_1}{dt} = c_{p1}p - e_{p1}x_1 \qquad 2.28$$

$$\frac{dx_2}{dt} = c_{p2}p - e_{p2}x_2 \qquad 2.29$$

$$\frac{dx_3}{dt} = c_{p3}p - e_{p3}x_3 \qquad 2.30$$

Equations 2.27-2.30 can be solved using the Ax=B matrix format as follows,

$$\begin{bmatrix} \dot{p} \\ \dot{x}_1 \\ \dot{x}_2 \\ \dot{x}_3 \end{bmatrix} = \begin{bmatrix} C_p & e_{p1}N_1 & e_{p2}N_2 & e_{p3}N_3 \\ c_{p1} & -e_{p1} & 0 & 0 \\ c_{p2} & 0 & -e_{p2} & 0 \\ c_{p3} & 0 & 0 & -e_{p3} \end{bmatrix} \cdot \begin{bmatrix} p \\ x_1 \\ x_2 \\ x_3 \end{bmatrix}$$

The eigenvalues (assuming exponential solutions) are found by finding the determinant of $|\lambda I - A|$ which is,

$$M = \begin{vmatrix} \lambda - C_p & -e_{p1}N_1 & -e_{p2}N_2 & -e_{p3}N_3 \\ -c_{p1} & \lambda + e_{p1} & 0 & 0 \\ -c_{p2} & 0 & \lambda + e_{p2} & 0 \\ -c_{p3} & 0 & 0 & \lambda + e_{p3} \end{vmatrix}$$

Expanding this matrix about the second row,

$$M = -c_{p1}\begin{vmatrix} -e_{p1}N_1 & -e_{p2}N_2 & -e_{p3}N_3 \\ 0 & \lambda+e_{p2} & 0 \\ 0 & 0 & \lambda+e_{p3} \end{vmatrix} - (\lambda+e_{p1})\begin{vmatrix} \lambda-C_p & -e_{p2}N_2 & -e_{p3}N_3 \\ -c_{p2} & \lambda+e_{p2} & 0 \\ -c_{p3} & 0 & \lambda+e_{p3} \end{vmatrix} + 0 + 0$$

After some algebra, the determinant gives,

$$\begin{aligned} &\lambda^4 + \lambda^3\left[e_{p2}+e_{p3}-C_p\right] + \lambda^2\left[e_{p2}e_{p3} - e_{p1}c_{p1}N_1 - C_pe_{p3} - C_pe_{p2} - e_{p2}c_{p2}N_2 - e_{p3}c_{p3}N_3\right] \\ &+\lambda^2\left[e_{p3}e_{p1} - C_pe_{p1} + e_{p1}e_{p2_1}\right] + \lambda\left[e_{p1}e_{p3}c_{p2}N_1 - e_{p1}e_{p2}c_{p1}N_1 - e_{p1}e_{p3}c_{p1}N_1 - e_{p2}e_{p3}C_p\right] \\ &+\lambda\left[-e_{p1}e_{p2}c_{p2}N_2 + e_{p1}e_{p2}(e_{p3}-C_p) - e_{p2}e_{p3}c_{p3}N_3 - C_pe_{p1}e_{p3} - e_{p1}e_{p3}c_{p3}N_3\right] \\ &+e_{p1}e_{p2}e_{p3}c_{p2}N_2 + e_{p1}e_{p2}e_{p3}C_p + e_{p1}e_{p2}e_{p3}c_{p3}N_3 + e_{p1}e_{p2}e_{p3}c_{p1}N_1 = 0 \end{aligned} \qquad 2.31$$

Upon substitution of C_p=-$c_{p1}N_1$-$c_{p2}N_2$-$c_{p3}N_3$, the form of 2.31 becomes $\lambda(\lambda^3+A\lambda^2+B\lambda+C)=0$. This means that the roots of 2.31 gives four modes (exponentials). Three of these modes have negative values for λ, and there is a DC-term (λ=0). Therefore, the time constants associated with the three deep levels can be found by measuring the decaying photocurrent.[10]

2.5 Modeling Results - Photoconductive Properties

Figure 2.3.2 shows the results of a numerical simulation based on the discussion in sections 2.1 - 2.3.[8] This code has been modified to include a third copper level (0.3 eV in figure 2.3.1). After irradiation from a 1.06 μm laser pulse long-lifetime electrons exist in the conduction band which gives rise to the on-state conductivity. After some time the second laser pulse stimulates band-band recombination, which extinguishes the electron current. This simulation can be operated to demonstrate how the material will behave under different excitation conditions. First, the idea of on-state conductivity saturation

will be explored. Next, the effects of the 2.1 μm laser pulse alone will be shown and discussed.

As described in section 2.4, the on-state conductivity of the switch is determined by the density of the Cu_B level and the laser pulse intensity. Figure 2.5.1 shows the numerical simulation of the material upon excitation from the turn-on laser pulse with various energies. This figure shows that the conductivity saturates as the laser intensity is increased. In section 2.4, it was shown that equation 2.21 is a good approximation for the on-state conductivity saturation. A comparison between equation 2.21 and the numerical code is shown in figure 2.5.2. In the numerical code, it was assumed that there are three copper levels present, and that an increase in the concentration of one of the copper centers leads to monotonic increase in the concentrations of the other copper centers. Over the limited range of concentrations considered here (1-5 x 10^{16} cm^{-3}), this assumption is considered reasonable. Therefore, figure 2.5.2 demonstrates that the approximation of equation 2.21 is reasonable for this case.

Next, the effects of excitation from the turn-off laser (2.1 μm) are described. In section 2.4, it was shown that an analytical model based on emission and capture at the various copper levels gives a solution that involves a sum-of-exponentials. The numerical code was altered to allow only the 2.1 μm laser pulse (figure 2.5.3) to excite the sample. The results of this simulation using several different doping densities are shown in figure 2.5.4. The decay times appear to increase with increasing copper density. It is also apparent that the photocurrent generated by the turn-off laser pulse has at least one slow time constant along with other fast time constants. The sum-of-exponentials result found in section 2.4 is therefore consistent with the numerical code.

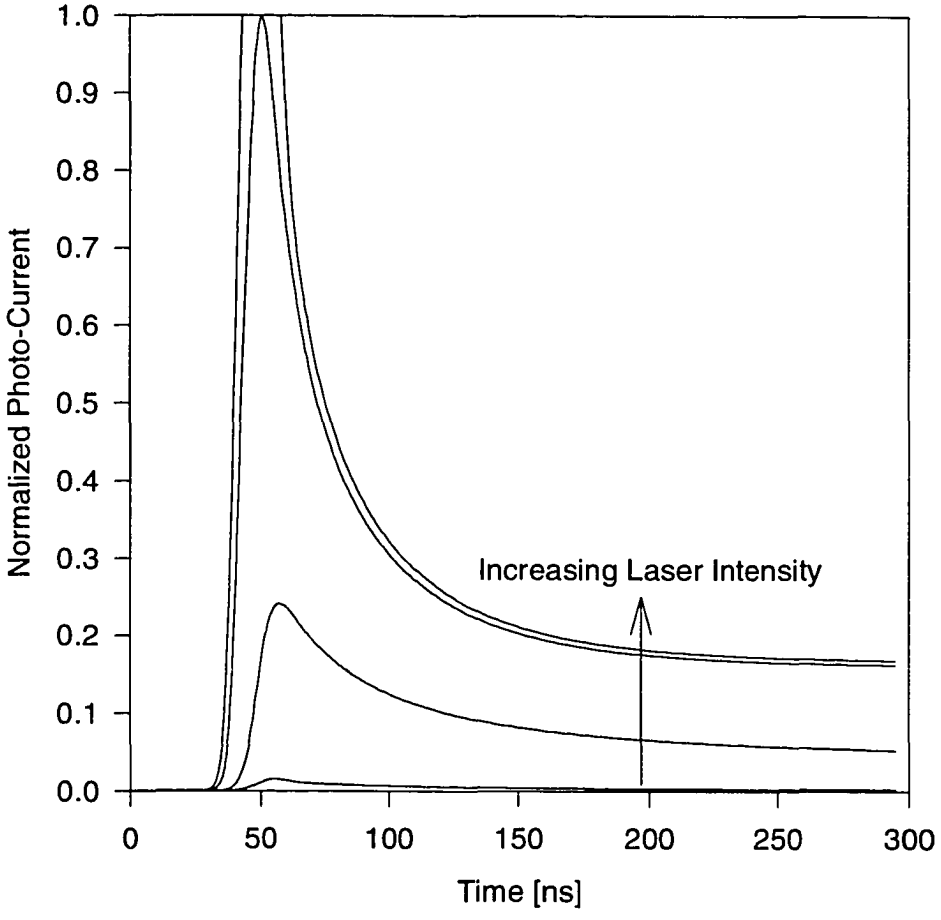

Figure 2.5.1. Numerical simulation of the IR-photoconductivity as a function of laser intensity using a 1.1 μm wavelength source.

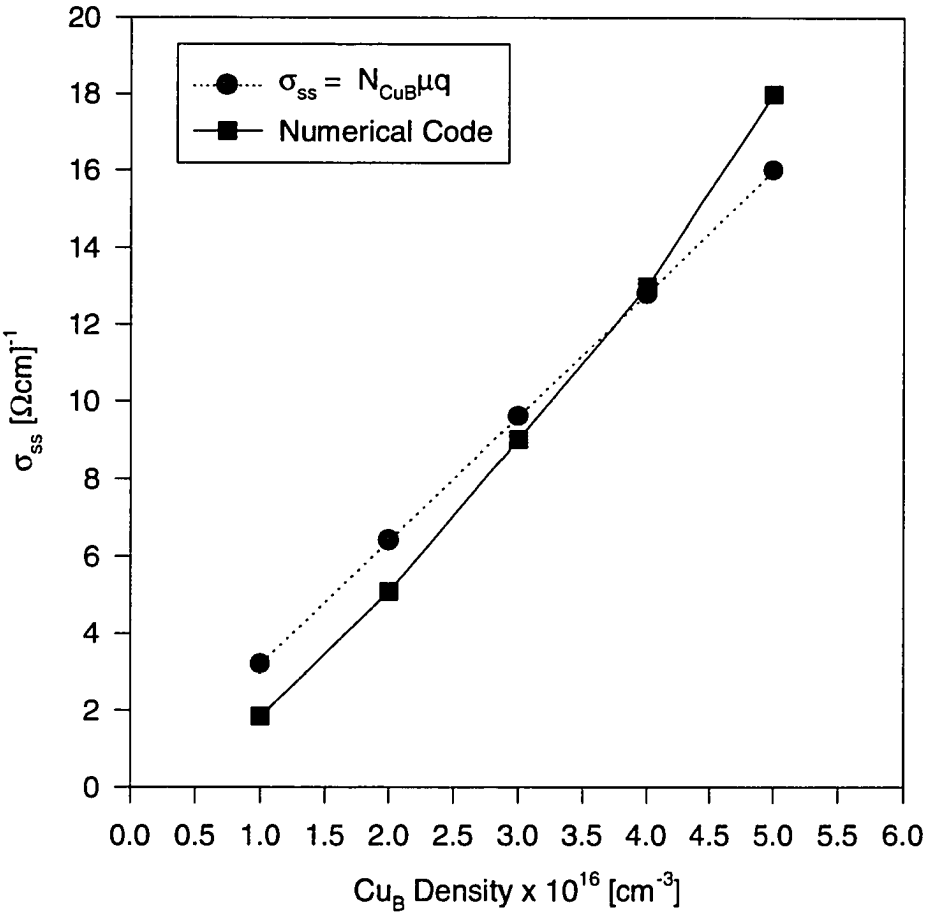

Figure 2.5.2. Comparison of the results of a linear model to the numerical code for the on-state photoconductivity 150 ns after the laser pulse ends.

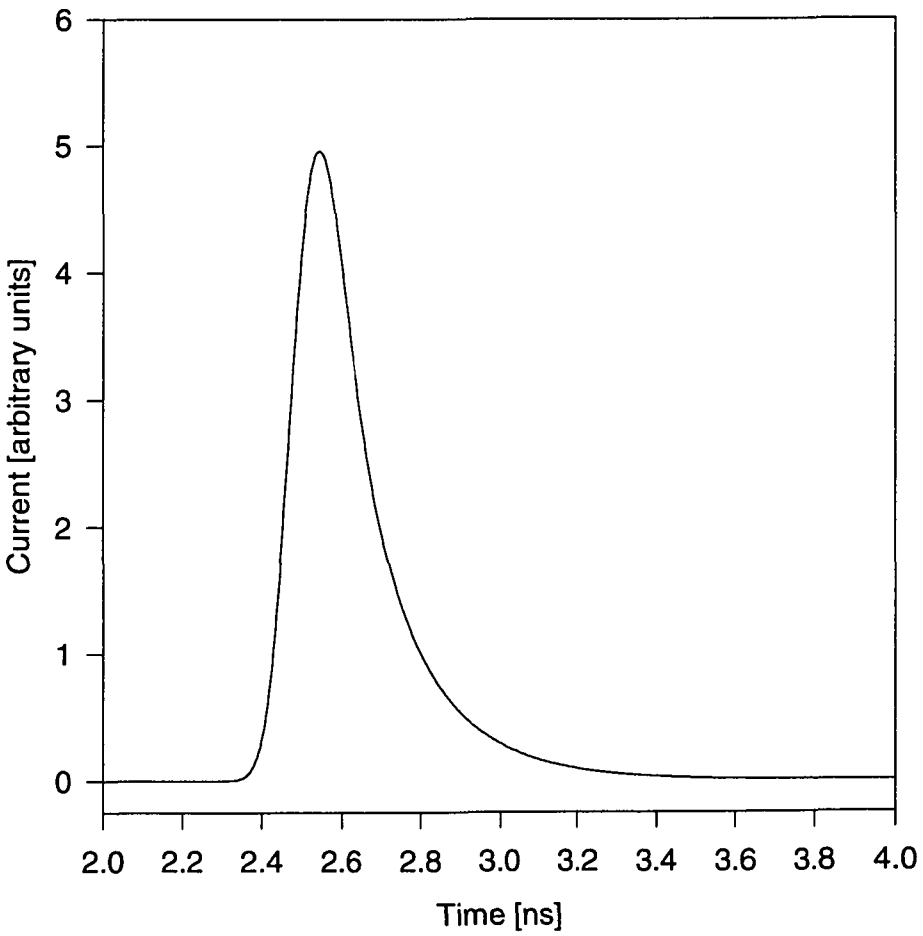

Figure 2.5.3. Model representation of the 2.1 μm laser pulse.

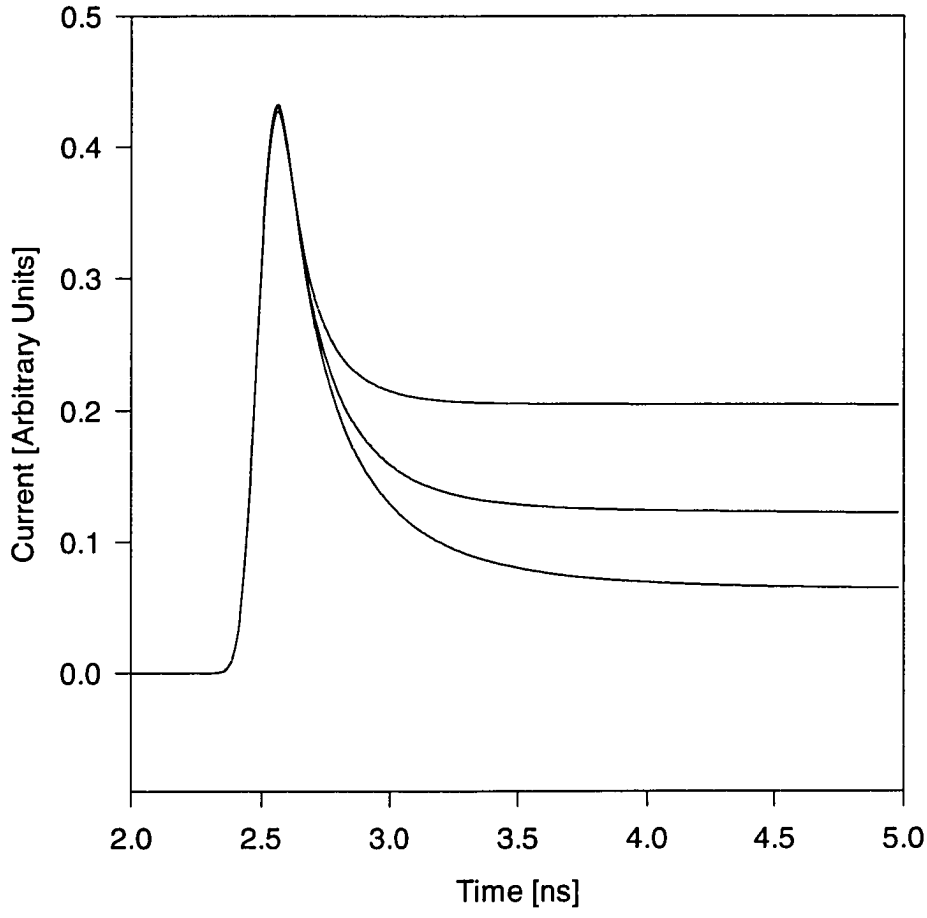

Figure 2.5.4. Model results for the excitation of the sample with the 2.1 μm laser source for different doping densities.

2.6 Electrical Compensation

In order to prove the validity of the assumptions in the model, gallium arsenide samples are prepared by copper diffusion such that the material is highly resistive and compensated.[5] The actual sample preparation is described in chapter 3, but in this section, a mathematical description of the compensation process is given. In a later chapter, the actual experimental results will be shown with a comparison to the model developed here.

Compensation of gallium arsenide is well established[12,13] using native defects such as EL2 and dopants such as chromium. Initially, the material doped with shallow acceptors or donors. Deep centers capture the free carriers and render them immobile, and therefore a low conductivity material is produced. An analytical model of this process can be developed starting with the charge neutrality condition,

$$p + \sum_m N_{Dm}^+ = n + \sum_n N_{An}^- \qquad 2.32$$

This condition means that the densities of free carriers (n, p) are offset by the densities of the trapped charges. In this case, there are m donors and n acceptors which are ionized, resulting in fixed positive and negative charges. The free charge densities are a function of the Fermi-level,

$$n = N_C \exp((E_F - E_C)/kT) \qquad 2.33$$

$$p = N_V \exp((E_V - E_F)/kT) \qquad 2.34$$

where N_C and N_V are the densities of state in the conduction and valence bands, E_F is the Fermi level, and E_V and E_C are the valence and conduction band energies. The fixed charge is represented by the fraction of ionized deep levels which is given using Fermi-Dirac statistics,

$$N_D^+ = \frac{N_D}{1 + e^{\frac{E_F - E_D}{kT}}} \qquad 2.35$$

$$N_A^- = \frac{N_A}{1 + e^{\frac{E_A - E_F}{kT}}} \qquad 2.36$$

where E_A and E_D are the activation energies of the acceptor and donor levels. The final equation to be used in this analysis is the mass-action law, $np = n_i^2$, in which the free charge carrier densities are related to the intrinsic carrier density, n_i. Now, multiplying equation 2.32 by n we get,

$$np + n\sum_{i=0}^{n} N_{D_i}^+ = n^2 + n\sum_{j=0}^{m} N_{Aj}^- \qquad 2.37$$

where, after re-arranging and using 2.35, 2.36, and mass action,

$$n^2 + n\left[\sum_{i=0}^{n} \frac{N_{A_i}}{1 + e^{\frac{E_{A_i} - E_F}{kT}}} - \sum_{j=0}^{m} \frac{N_{D_j}}{1 + e^{\frac{E_F - E_{D_j}}{kT}}}\right] = n_i^2 \qquad 2.38$$

This is a quadratic equation in n, and can be solved numerically by adjusting the Fermi level until the right-hand-side equals the left-hand-side. Any number of levels may be added to the system (acceptors or donors). The Fermi-level is used to calculate the free carrier density, and the mass action law is used to calculate the opposite carrier density. Therefore, the conductivity may be calculated using,

$$\sigma = q(n\mu_n + p\mu_p)^{-1} \qquad 2.39$$

One assumption to be made here is that the mobility (μ) is not a function of the doping densities, which is definitely not the case. The effect is to reduce the conductivity at

higher doping densities, and the maximum change in the mobility may be only a factor of two or three. Since the compensation curves will involve conductivity swings of many orders of magnitude, the effects of the change in mobility will be ignored. This analysis has been implemented into a Turbo Pascal code to give the compensation curves for gallium arsenide of various doping profiles. This code is given in Appendix A.

The results of the above analysis are given in a series of curves which show the effect of adding donors and acceptors to the material. Figure 2.6.1 shows the compensation curve for the case of one shallow donor and one deep acceptor. The compensation point occurs when the donor and acceptor densities are equal ($5x10^{16}$ cm^{-3}). Also, the Fermi-level becomes pinned at the deep acceptor level, and therefore the conductivity is low. It should be noted that the intrinsic limit of this material is about 10^{-9} $(\Omega cm)^{-1}$, and therefore the minimum in the compensation curves cannot be lower than this limit. The addition of another donor and acceptor to the system causes the compensation curve to change to that shown in figure 2.6.2. Here, there are two donors (densities of $1x10^{16}$ cm^{-3}) and two acceptors ($1x10^{16}$ cm^{-3}), and it is shown that there are two effective compensation points at which the Fermi-level shifts toward the deepest level in the system. Also, it is apparent that the range over which very low conductivities are observed is smaller in this case. Figure 2.6.3 shows the compensation curve for the case of three acceptors and one donor. The compensation point at which the total acceptor density equals the total donor density is still obvious, but the conductivity rises more gradually due to the added deep acceptor level. These curves are generated to show that the compensation curve changes dramatically when the deep level configuration is altered.

This model will be used in Chapter 4 to demonstrate how the deep levels change due to various sample processing parameters.

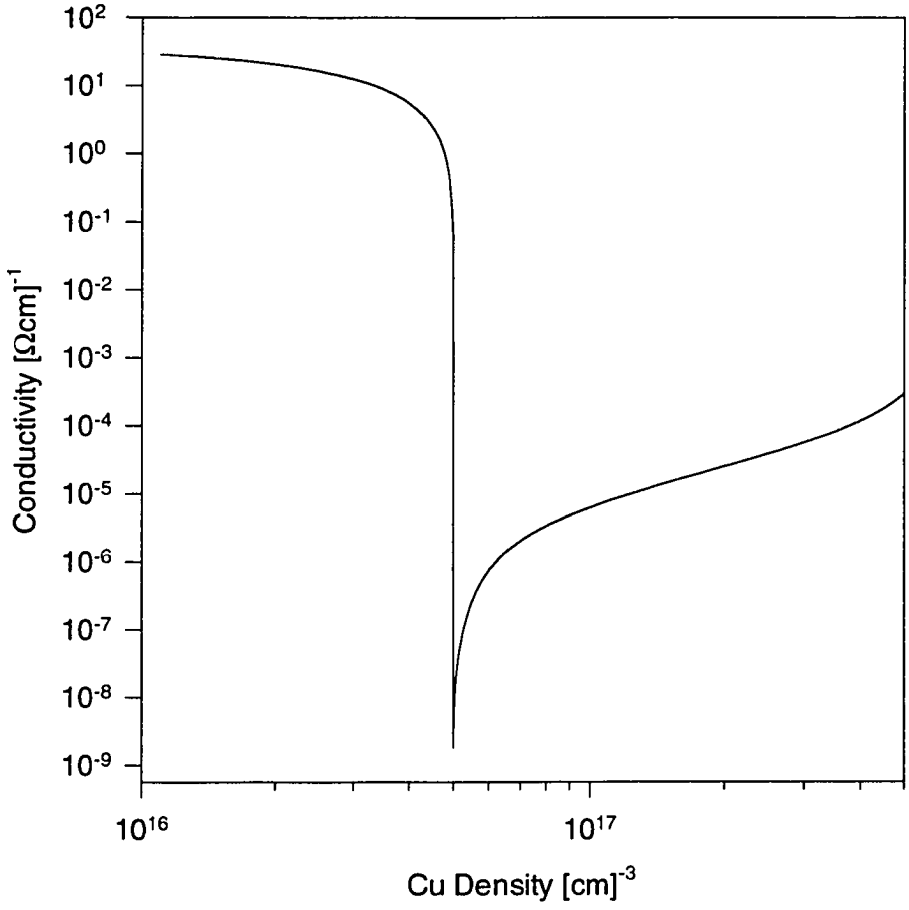

Figure 2.6.1. Compensation model results for one deep acceptor and one shallow donor.

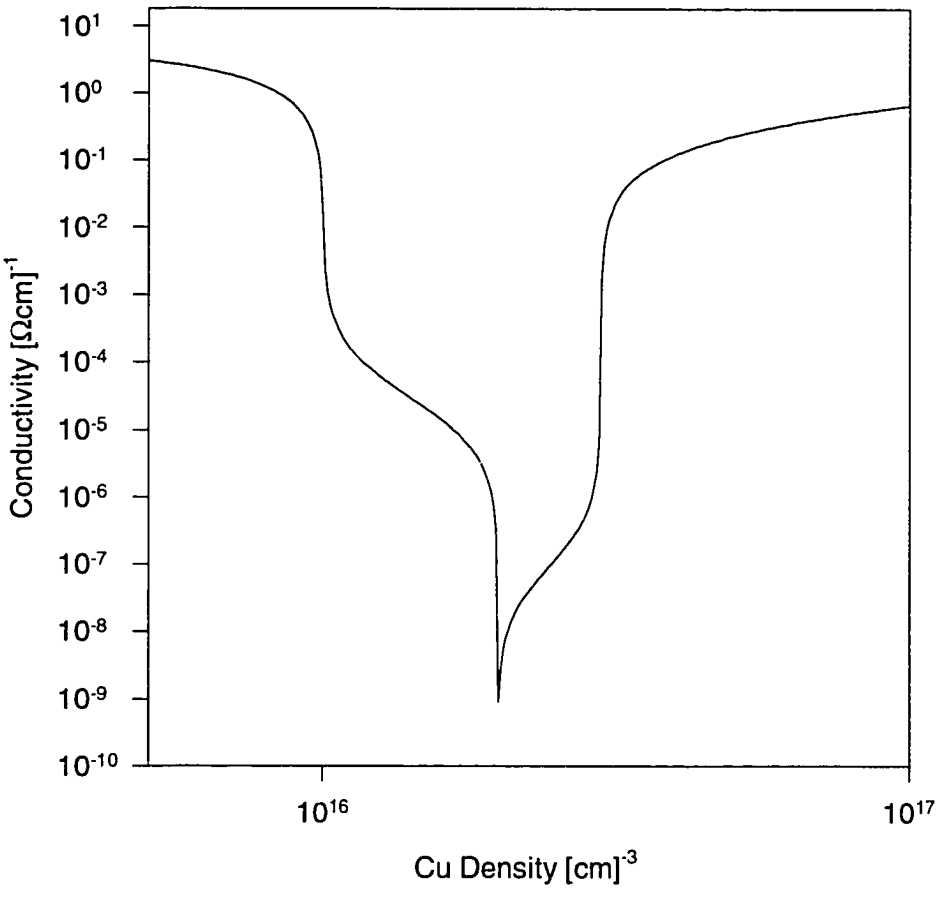

Figure 2.6.2. Compensation curve for three donors and one deep acceptor.

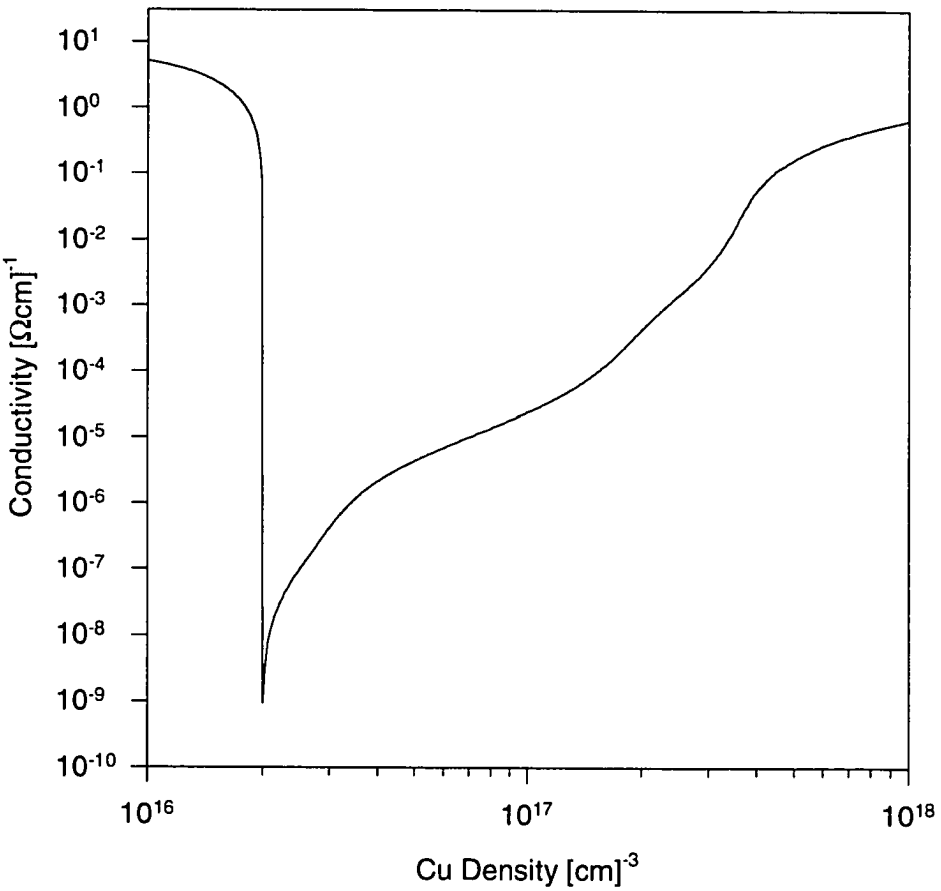

Figure 2.6.3. Compensation curve for three deep acceptors and one shallow donor.

CHAPTER 3

SAMPLE PREPARATION

The material of interest in this work is copper-doped gallium arsenide.[14-18] Typically, a gallium arsenide wafer is plated with copper using a sputtering or thermal deposition system, and then the wafer is placed in a sealed reaction tube. The tube is then placed into an oven at a fixed temperature for a given amount of time. Upon extraction from the oven (and tube) the wafer is then polished, and electrical contacts are then applied. This process has been successfully implemented in the development of BOSS devices as well as material used in studies performed elsewhere.[2,3] In these previous studies, it appears that little or no attention has been given to the uniformity of the copper diffusion, which is of great importance in device manufacturing. Also, the activation energies associated with these copper impurities are shown to be nonuniformly distributed.

3.1 Diffusion

The origins of formation of many important deep levels in gallium arsenide are still under some scrutiny, but it is believed that copper levels are formed by a combination of copper substitutionals (copper on a gallium site) and arsenic vacancies/interstitials.[14,15,17] Copper diffuses interstitially very quickly, after which the slower process of formation of

substitutional copper occurs. In order to check the typical time constants, the diffusion equation is solved,

$$\frac{\partial N}{dt} = \nabla^2(DN) \qquad 3.1$$

where N is the density of the impurity. The diffusion coefficient (D) can be considered to be independent of depth when the dopant concentrations are below about 10^{18} cm^{-3} which is the case here. This diffusion coefficient can be considered to be a combination of two diffusion coefficients to account for both the fast interstitial diffusion and slow substitutional diffusion. The initial condition is N(x,0) = 0 , and the boundary conditions are $N(0,t) = N_0$ and $N(\infty,t) = 0$ for an unbounded, one-dimensional geometry. The solution is the complimentary error function (for lengths much greater than a diffusion length),

$$N(x,t) = N_0 \frac{2\sqrt{Dt}}{\pi x} \exp\left[-\frac{x^2}{4Dt}\right] \qquad 3.2$$

where N_0 is the concentration of dopant which exists at the boundary for all times (infinite supply). This allows us to calculate the diffusion times required to ensure that the copper is uniformly distributed across the sample thicknesses of interest here (0.5 mm - 1.0 mm) as shown in figure 3.1.1. Notice that diffusion from both sides of the sample is considered. Also, it is important to note that the copper distribution is fairly uniform after about 15 minutes, which means that the copper diffuses fairly rapidly.

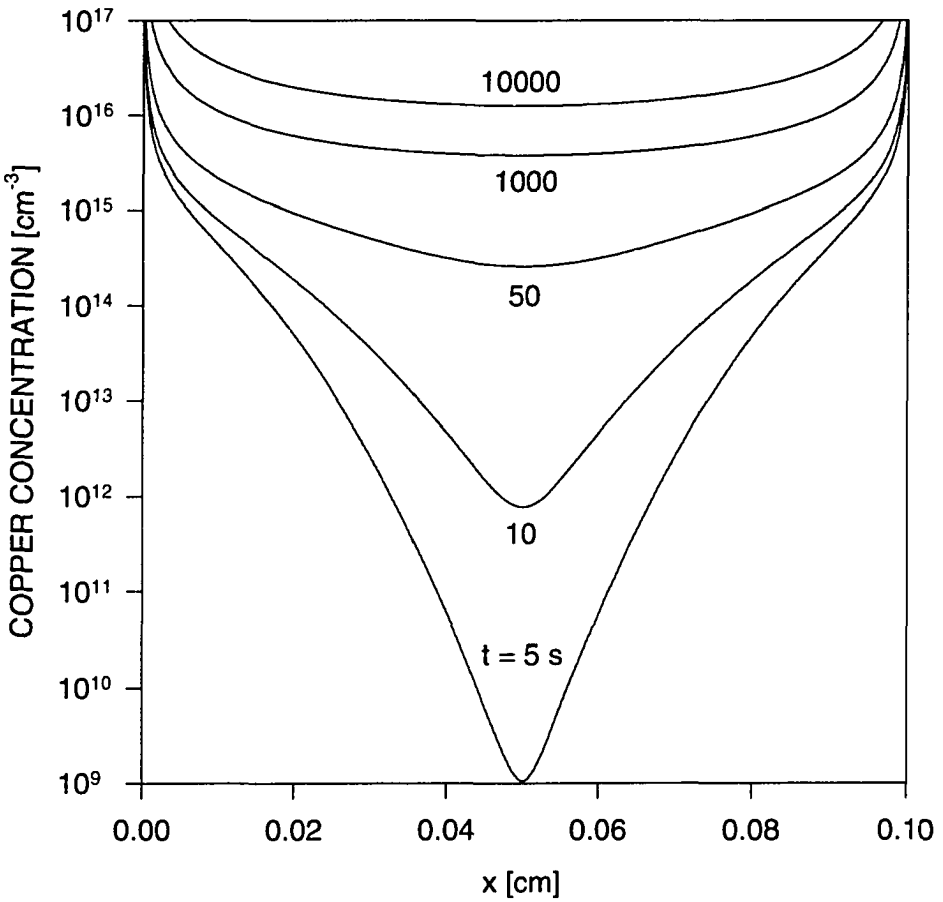

Figure 3.1.1. Model of the spatial diffusion profile for various diffusion times.

3.2 Vapor-Phase Diffusion

Diffused copper is known to precipitate in gallium arsenide[11] which leads one to believe that non-uniform copper distributions will be obtained. Also, the technique of plating the wafer with copper causes inherent inhomogeneities in the boundary conditions. The flow of arsenic into and out of the wafer during the diffusion process is critical in the formation of the deep levels associated with copper as well as native defects. Therefore, the copper plate, which cracks and wrinkles during diffusion, is not adequate to allow uniform flow of arsenic.[19-21] Observations of the poor surface-quality of the copper plate after diffusion confirm that the boundary conditions are not uniform during this diffusion process.

The boundary conditions in such a system are very important in that they determine, perhaps predominantly, the relative uniformity of the copper density in the bulk of the wafer. It has been noted that a copper cap on the wafer effectively inhibits the in- or out-diffusion of arsenic, and the copper layer can crack and lift off the wafer.[20] An alternative to copper capping is a vapor-phase diffusion. This involves the system drawn in figure 3.2.1. The sample is placed in the ampoule along with solid sources of copper and arsenic. The idea is that during the anneal, the copper and arsenic sublimate and provide adequate sources in the vapor phase. Arsenic sublimates completely at the pressure and temperatures used here, but copper only partially sublimates. The concentration of copper required for diffusion into the crystal, however, is only around 10^{17} cm^{-3} which is not difficult to obtain. The goal of this work is to develop a system in which the experimental parameters can be varied in order to find trends. One experiment

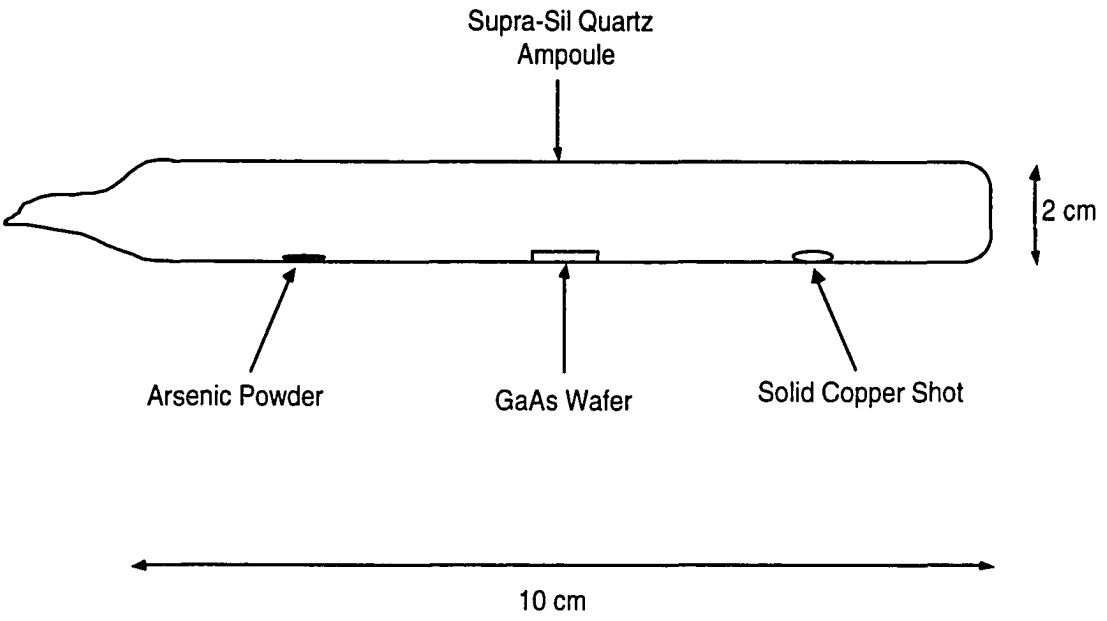

Figure 3.2.1. Ampoule used for the vapor-phase diffusion process.

of interest is to vary the arsenic partial pressure in the ampoule. This allows the concentrations of arsenic-related defects in the crystal to be varied. In order to carry out such a study, the nature of the interaction between copper and arsenic vapor and solids must be explored. Copper and arsenic form two main compounds: Cu_3As, and Cu_5As_2. At atmospheric pressure Cu_3As melts at about 800 °C, which means that at the lower pressures in the ampoule, this compound may be formed readily. The Cu_5As_2 is more robust, however, and may be a solid for the experimental conditions used in this work. The appearance of Cu_5As_2 may be observed as a rust/orange-colored film or deposit that forms in the ampoule during or after the anneal. The formation of either of these compounds extracts from the arsenic in the vapor phase, and thus must be considered in the calculation of the arsenic partial pressure.

Experiments have been performed to determine the nature of the interaction of copper and arsenic during the anneal. Ampoules were placed in the furnace at temperatures ranging between 500-600 °C with solid sources of copper and arsenic inside. The copper source was a quartz pellet coated with a 1 μm thick layer of copper which was applied using an RF-sputtering system. The ampoules are made of Supra-Sil Quartz, and they are prepared by a glass-blower. A drawing of the manifold is shown in figure 3.2.2. The arsenic source, copper source, and GaAs samples are placed into the tubes which are attached to the manifold, and then the manifold is connected to a vacuum pump which pumps the tubes down to about 10^{-5} Torr. During the pumping process, the ampoules are slightly heated with a torch in order to vaporize and extract any water that may be left in

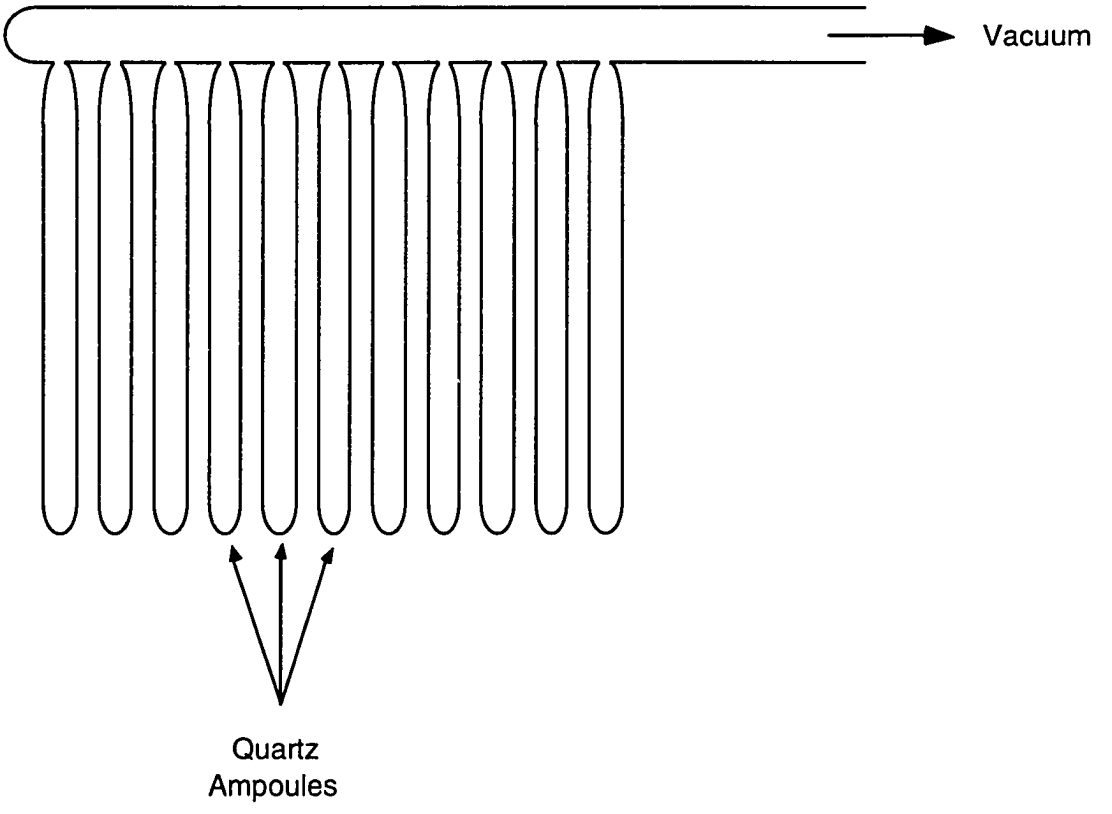

Figure 3.2.2. Manifold on which ampoules are loaded, evacuated and sealed.

the tubes. After the tubes reach the desired pressure, the ampoules are detached from the manifold using the hydrogen torch and left to cool.

The arsenic source in the ampoules was a powder form that was weighed and placed into the ampoule. With no arsenic in the ampoule during the anneal, the copper layer remained on the quartz pellet with some copper vaporizing and plating-out on the tube wall. This implies that a significant amount of copper is in the vapor-phase during the anneal. Next, a small amount of arsenic (2 mg) added to an ampoule along with the copper source (3 mg), and after the anneal the quartz pellet had the flaky rust/orange coating with the inside of the ampoule coated with the same substance. This is consistent with the formation of Cu_5As_2.

Arsenic vapor in the ampoule forms either As_2 or As_4, and the relative concentration of these molecules depends on the temperature. At temperatures below about 1000 C, the arsenic is typically assumed to be comprised of As_4 vapor.[22,23] In order to control the arsenic out-flow from the wafer during diffusion, the arsenic partial pressure must be controlled. In order to calculate this pressure, the ideal gas law is assumed,

$$p = \frac{\overline{R}T}{vM} \tag{3.4}$$

where the Rydberg constant is $R=\overline{R}/M$ ($\overline{R}$ = 8.3144 kN·m/kmol·K), $\overline{v}$ is the specific volume (m^3/g), and M is the molarity (g/mol). Using an ampoule of the size shown in figure 3.2.1, the specific volume is 1.62×10^{-3} m^3/g. The molarity, M, is 74.9 g/mol, and therefore the partial pressure for As is 438 Torr at 580 °C and 12 mg As. This means that the As_2 pressure is 219 Torr, and As_4 pressure is 109 Torr.

3.3 Role of Arsenic Pressure

Controlling the concentration of arsenic vacancies and/or interstitials is important in the formation of typical arsenic related defects. With respect to copper impurities, the arsenic defects may play a role in the structure of the various copper defects. Some possible defects in gallium arsenide are gallium vacancies V_{Ga} , arsenic vacancies, V_{As}, gallium antisite, Ga_{As} (gallium on arsenic site), gallium interstitials, Ga_i, and arsenic interstitials, As_i. Combinations of these defects can produce a wide range of possibilities such as, $V_{Ga}V_{Ga}$, Ga_iV_{Ga}, $V_{Ga}V_{As}$, $As_{Ga}V_{As}$, As_iV_{As}, and so on. The possibilities becomes even more complicated by the addition of another constituent such as copper where copper related complexes can occur ($Cu_{Ga}V_{As}As_i$, etc.). The energy of formation of defects has been ranked by Milnes[24] as,

$$U_{Ga_i} > U_{V_{As}} > U_{V_{Ga}} > U_{As_i} \qquad 3.5$$

which means that arsenic interstitials are relatively easy to form and must be considered.

Upon heat treatment at about 1000 °C for 67 hours, Nishizawa[25] observed an acceptor density - arsenic pressure dependence which shows a distinct minimum in the acceptor density at a given arsenic pressure. This minimum appears to be lower at the lower annealing temperature of 900 °C, which means that the effect may be observed at much lower arsenic pressures with lower temperatures. The minimum observed in the data is explained by Frenkel defect formation in which a gallium atom is ejected leaving a gallium interstitial and a vacancy (similarly for arsenic). The ambient arsenic pressure will determine the ratio of arsenic vacancy concentration (denoted $[V_{As}]$) to arsenic interstitial concentration, $[As_i]$. Mass action requires,[23]

$$[V_{As}][As_i] = Cons\tan t \qquad 3.6$$

Since arsenic atoms diffuse from the crystal easily while gallium atoms diffuse very slowly, we need not consider a relationship similar to 3.6 for gallium. Gallium Frenkel defects can, however, form such that $[Ga_i] = [V_{Ga}]$. If the arsenic pressure is adjusted such that $[V_{As}] = [As_i]$, then a situation may arise where gallium interstitials do not have arsenic sites on which to reside (upon cooling). This means that defects formed by Ga_{As} will be excluded in such a situation, and therefore a minimum in the acceptor density is observed. Of course, further increase in arsenic pressure will cause other defects to form which will raise the acceptor density. Assuming that As_4 is the predominant gaseous form of arsenic at the temperatures considered here, then the reaction of gallium arsenide and the arsenic vacancies follows,

$$4GaAs(s) \Leftrightarrow 4Ga(s) + 4V_{As} + As_4(g) \qquad 3.7$$

where (s) stands for solid and (g) stands for gas. This interaction is considered to be the dominant mechanism by which arsenic vacancies are formed at temperatures less than about 700 °C.

The scenario described above is an example of the importance associated with the role of arsenic pressure in the experiments. A complete knowledge of the interaction of arsenic related defects with the lattice in forming deep and shallow levels is not nearly available. However, some experiments have been carried out in the past to show some interesting effects.[22-25] Typically, a gallium arsenide wafer is heat-treated in the presence of a known arsenic vapor pressure. Hall measurements are performed to determine the carrier concentrations, and/or possibly DLTS (or PICTS) measurements are used in order

to determine the effect on the deep/shallow levels of the arsenic pressure.[26-30] It is established that copper acceptors are associated with arsenic vacancies.[20,21]

3.4 Electrical Contacts

The application of Ohmic contacts to gallium arsenide has been studied extensively over the past 20 years. Some of the best early work with contacts for GaAs bulk-effect devices was performed by Braslau at IBM in the late 1960's.[31] The use of alloyed Au, Ge, and Ni to form Ohmic contacts to the wafer surface is a technique still in wide use today.[32-35] The alloy of Au and Ge is eutectic at a melting temperature of about 330 °C, but small droplets are formed causing a non-uniform contact. It has been shown that the Au-Ge formulation provides an excellent n^+ layer, and a film of Au-Ge can be easily applied using thermal evaporation or RF-sputtering. The idea is that the gold acts as a getter, and the germanium becomes a substitutional, shallow donor in the lattice on a gallium site. In order to have specific contact resistances below $2x10^{-6}$ Ωcm^2, the germanium must be almost exclusively on a gallium site with electrically active densities on the order of 10^{19} cm^{-3}. Similarly, a contact to p-type gallium arsenide can be made using gold-zinc (Au-Zn). This formulation uses zinc substitutionals on gallium sites in order to provide a p-type dopant to the contact layer. In addition to the Au-Ge or Au-Zn layers, some have used a thin (10-100 Å) under-layer of nickel in order to improve wetting. A robust contact formulation is 50 Å Ni, 2000 Å Au-Ge, and a 5000 Å Au cap. It has also been shown that non-alloyed contacts are also very good for microelectronics applications.

The interface between the Au-Ge layer and the GaAs wafer has been shown to have 'spikes' extending from the Au-Ge into the wafer upon alloying. These spikes are on the order of micrometers, and act as the primary ohmic contact regions. The problem with this scenario is that high electric fields can develop around these spikes which causes excess stress. Perhaps more important is the fact that the current will be constricted to these spike channels, and therefore the current densities may become high enough to cause damage. A solution to this problem is the use of ion implantation to smooth the contact region. The idea is to implant silicon ions (for example) into the region on which the contact is to be placed. Upon activation of the implant, a metalization can be deposited onto the heavily n-type region. This allows the use of either Au-Ge or other metallizations in order to create a smooth contact region. This technique also allows the use of refractory metals in the contact formulation which permits the device to operate at higher temperatures.

3.5 Present Work

In this work the wafers were prepared using the closed-tube system shown in figure 3.2.1. A Lindberg, three-zone tube furnace was used to anneal the samples. The temperature distribution across the oven hot-zone is shown in figure 3.5.1. A typical ampoule length is about 10 cm, and therefore the temperature distribution across the ampoule during the anneal is constant to within about 1%. For safety, the ampoule is placed in an outer tube which is sealed and connected to a pressurized nitrogen-gas bottle

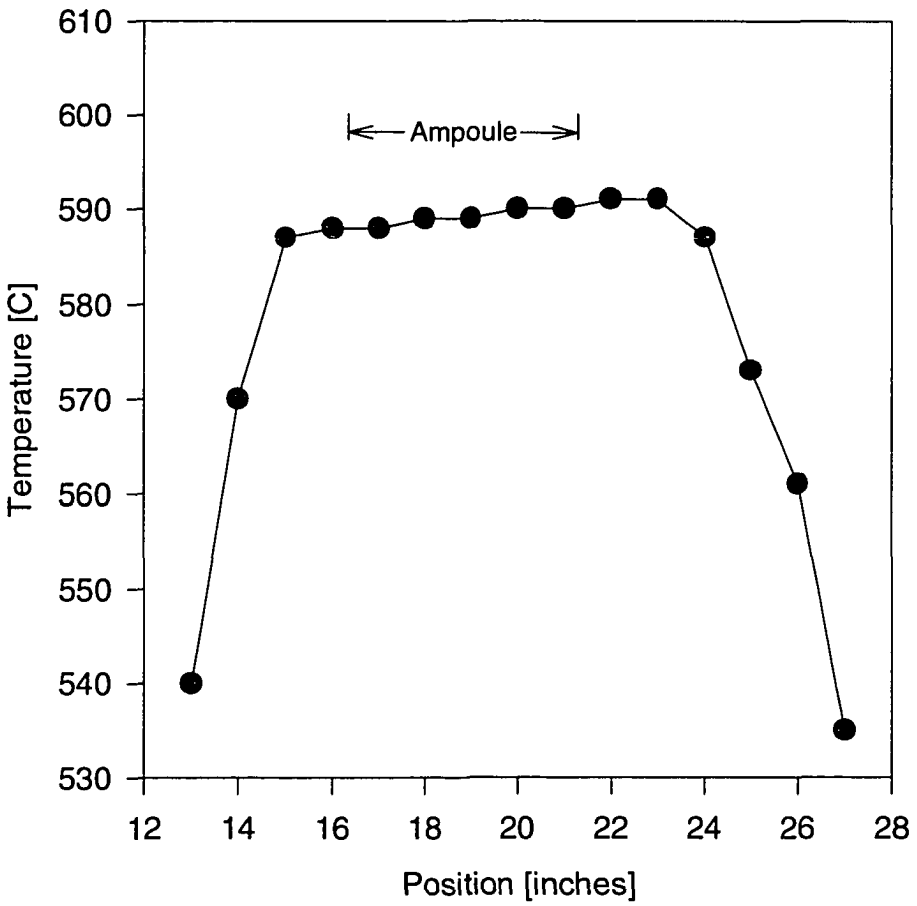

Figure 3.5.1. Temperature across the furnace tube hot-zone.

and a vent system. In case of ampoule breakage, the sealed outer tube is then purged with flowing nitrogen which is exhausted through an oil bubbler in order to remove any arsenic.

After annealing the ampoule, the wafer is removed by inscribing a small etched line to the ampoule surface perpendicular to the length and then manually breaking the ampoule along this etch. Care must be taken so as not to break the contained wafer during this process. Upon removal from the ampoule, observation of the wafer surface reveals contamination by deposits created during the cooling of the ampoule. These deposits are a combination of arsenic-copper compounds described earlier. The surface must be cleaned and polished before the electrical contacts are applied to the GaAs surface. First the sample is lapped using a series of lapping films (30 μm to 1 μm). Next, the samples are placed in a laminar flow polishing system which uses a bromine-methanol (1% Br) solution. This system results in polished surfaces with etch pits of sizes less than 1 μm which is quite adequate for the application of electrical contacts.

The electrical contacts are Au:Ge for an n-type contact, and Au:Zn for a p-type contact. If the wafer is to be used for optically activated switching work in which the electrical current during the on-state consists of electrons, then the contacts are n-type (even if the wafer is p-type in the off-state). If however the sample is p-type and to be used for Hall measurements, then the contacts to be used are Au:Zn (p-type). It is also advantageous in some cases to use both Au:Ge and Au:Zn to form a p-i-n structure on highly resistive wafers. The technique for the application of the contacts uses an RF-Sputtering system, which uses a discharge in argon to accelerate ions to the sputtering target. The advantage of using an RF-discharge instead of DC is that dielectrics can be

used as targets in the RF-system. The reason that dielectrics cannot be used in the DC-system is that any dielectric will act as a capacitor which charges and causes the discharge to be extinguished. The RF-discharge uses the displacement current on each cycle in order to maintain the discharge. This allows the use of dielectric masks on the wafers for several purposes. A common technique for diffusion masking is to apply a layer of silicon nitride to the surface before the diffusion. Also, in discharge systems the wafer surface can be cleaned under high vacuum by performing a reverse etch. This allows the sample surface to be etched to a known depth which removes any oxides or contamination. Cleaning the sample outside the vacuum is not very effective because contaminants from the ambient build up at a rate of about one monolayer per minute.

After the electrical contacts are applied to the sample surface, contacts must be made to the external circuit. The most durable connection is a simple pressure-contact where a wire is pressed against the gold contact, but this method is not optimum due to current crowding and oxides that can build up. Solder can be used on Ni:Au:Ge or Ni:Au:Zn contacts, but the excess heat of the solder tip is not desirable. The contacts or the bulk material can be damaged during the soldering process. The best method used to date employs silver epoxy to connect a wire or metal strip to the semiconductor. This epoxy is simply a base resin and hardener which has silver powder mixed into both. Upon mixing, the epoxy requires a short (15 minute) anneal at about 150 C. Figure 3.5.2 shows the final sample connection scheme.

After the electrical contacts are applied, the sample is ready for testing. The first test performed is designed to check the quality of the contacts. A curve tracer is used to

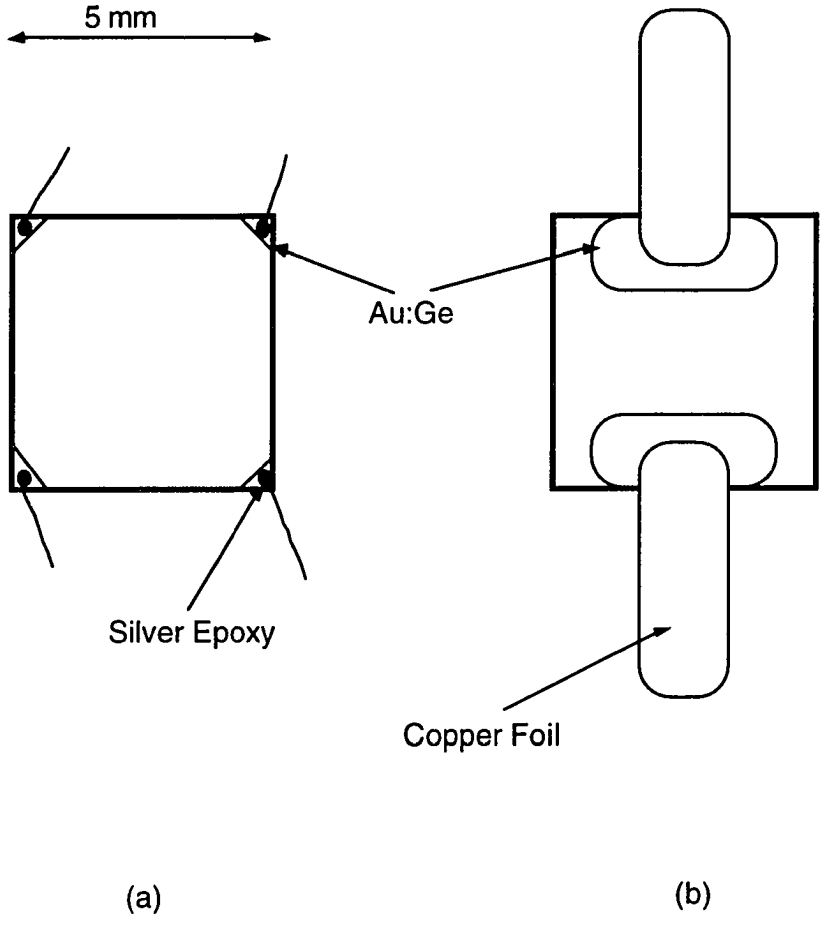

Figure 3.5.2. (a) Hall and (b) strip-line contacts used in the experiments.

determine if the contacts are Ohmic or rectifying. This, of course, can only be adequately done for lower resistance samples because the contact junction resistance may be dominated by the bulk for highly resistive samples. If the sample resistance is greater than a few kilo-Ohms, than DC current-voltage measurements are made in order to determine the linearity of the sample resistance. Typically, if the sample shows any non-linearity, then the contacts are lapped and polished away and new contacts are applied. In this way, linear Ohmic contacts are formed on each sample before any characterization experiments are performed.

CHAPTER 4

COMPENSATION

In chapter 2 (section 5), the compensation process was described using an analytical model. This model uses charge neutrality and Fermi-Dirac distribution functions in order to demonstrate the compensation technique. In this chapter, the experimental approach to compensation of silicon-doped gallium arsenide will be described. Given that silicon is predominantly a shallow donor in gallium arsenide, it is then necessary to use a deep acceptor for compensation. Silicon is an amphoteric dopant in GaAs, but the preferred state is that of the donor, Si_{Ga}.[36] It has been demonstrated that heat treatments of Si-doped GaAs can cause silicon site switching which leads to the formation of the acceptor, Si_{As}.[37] Copper is a deep acceptor which is required for the operation of the BOSS devices described in previous chapters, and therefore the diffusion of copper into gallium arsenide will be a major concern in this work. Also, the effects of heat treatment on the gallium arsenide with and without copper will be explored. The idea is to experimentally define the compensation curves shown in the modeling section (2.5), and to demonstrate refined techniques for processing of heat-treated gallium arsenide.

4.1 Copper Diffusion and Compensation

The wafers described in this section were all processed according to the steps outlined in section 3.5. The experiments given here are designed to describe the compensation process for several different silicon doping densities. Using a thermal diffusion technique, the copper concentration can be varied by simply changing the temperature of the anneal.[5] As described in chapters two and three, when the copper concentration is adjusted via annealing temperature, the copper concentration increases and eventually becomes comparable to the silicon density. Complete compensation occurs when the copper and silicon densities are equal, and therefore, the sample becomes highly resistive electrically. Beyond this compensation temperature, the excess copper causes the sample to be p-type. In order to measure these effects and determine consistency, the samples are 1 cm x 1 cm square, and they are cut into four squares after the copper diffusion and polishing steps. This allows nearly identical samples to be tested under different conditions. Each ingot from which the samples were taken was prepared by Bertram Laboratories with a specified silicon doping density. Doping densities in the low 10^{16} cm^{-3} are difficult to obtain because this is the lower limit of the boat grown technique. Therefore, there is a silicon density gradient across the length of the ingot of about a factor of 2.5. This means that one ingot supplied two significantly different silicon doping densities. The goal is to demonstrate compensation with four different silicon doping densities (1, 2, 6, 70 x 10^{16} cm^{-3}). The wafer names are associated with the silicon doping density in Table 4.1.

Table 4.1. Identification of wafers used in the experiments.

Ingot # - Wafer #	Si-Density $10^{16}[cm]^{-3}$
88-89	1
88-68	2
22-23	6
57-21	70

Copper doping of samples from wafer 89 was performed according to the procedure described in chapter 3. The samples were placed in the evacuated quartz ampoules, and the ampoules were annealed for eight hours in the three-zone tube furnace. The temperature in the furnace is constant (± 2%) over an eight inch range. This means that the temperature was held constant across the entire six-inch ampoule. The temperature at the sample location was measured using a type-K thermocouple. Upon extraction from the oven, the ampoule was allowed to cool in air for several minutes before being broken in order to remove the sample.

Figure 4.1.1 shows the compensation curve for this wafer.[5] The conductivity of the samples decreases with increasing temperature, which is an indication that the increasing copper density is providing the necessary deep copper centers needed for compensation. At about 553 °C, there is a dramatic drop in conductivity demonstrating that the copper concentration is very nearly equal to the silicon concentration at this temperature. Further increase in the temperature (ie. copper concentration) causes the conductivity to begin elevating. This is due to the excess copper acceptors, and the much more gradual slope is due in part to the lower mobility of holes as compared to electrons. It is interesting to note that as the copper concentration approaches the silicon concentration, the spread in the data points increases. Remember that a 1 cm x 1 cm sample is prepared and separated into four samples, thereby providing some statistical significance. In fact, at a temperature very near the compensation point, a difference in conductivity of more than two orders of magnitude was observed for identically prepared

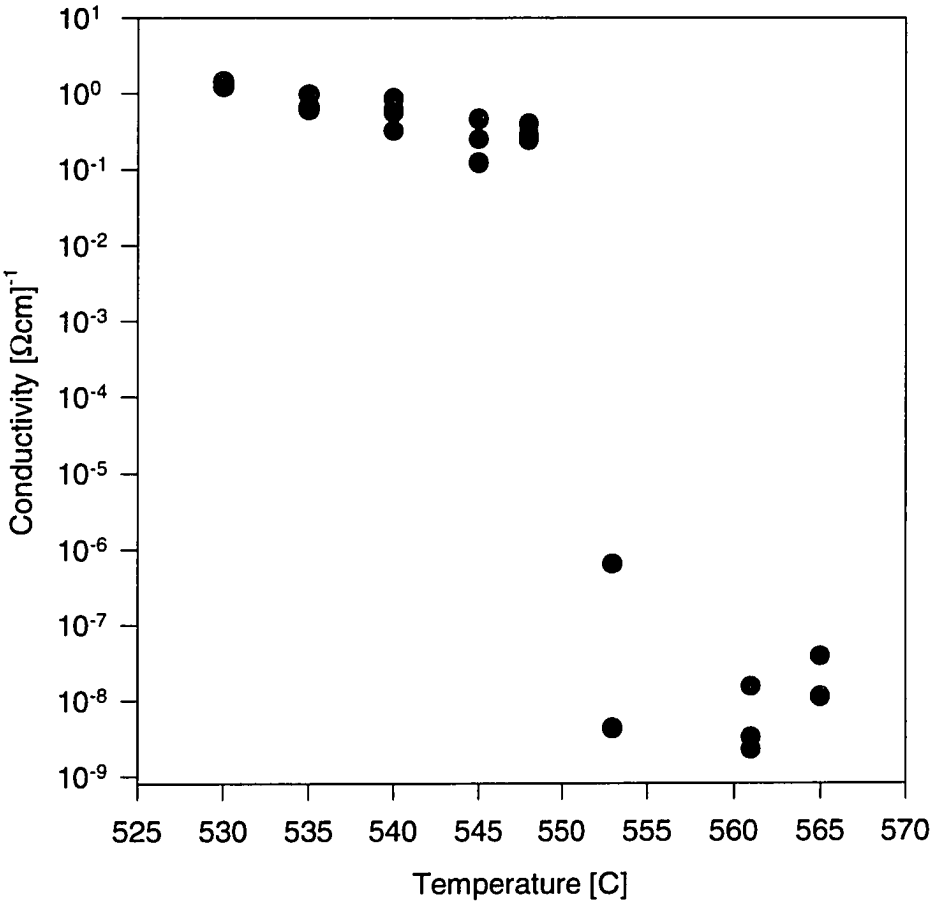

Figure 4.1.1. Compensation curve for wafer #89.

samples. This shows the sensitivity of the electrical characteristics (non-uniformity) near the compensation point.

Wafer 68 of the same ingot had an initial silicon concentration of about $2x10^{16}$ cm^{-3} . The compensation curve for this wafer is similar to that of wafer 89, but in this experiment, several compensated samples were prepared with different arsenic masses in the ampoule during the diffusion. The significance of changing the arsenic partial pressure was described in chapter 3, and figure 4.1.2 demonstrates the effect on the electrical properties of changing the arsenic pressure. The idea is that shallow acceptors are formed preferentially when the arsenic partial pressure is low. This leads to the conclusion that arsenic vacancies are involved with the shallow copper acceptors or some other arsenic related acceptor. The arsenic partial pressures in the ampoule are calculated based on the assumption that arsenic sublimates into As_4.[23,38] At the compensation temperature, the arsenic partial pressures are approximately 13, 106, and 796 Torr. These calculations assume no reaction between the copper and arsenic as discussed in chapter 3. The experiments show that the lowest conductivity was obtained with the highest arsenic mass in the ampoule for this wafer. The conductivity was about 0.4 $(\Omega cm)^{-1}$ for a sample annealed with no arsenic in the ampoule. This leads to the assumption that the shallow copper centers are related to an arsenic vacancy, or the deep copper centers are related to interstitial copper. It should be noted that the conductivities were calculated from resistance measurements which were taken using a Keithley 617 electrometer. An I-V curve was generated for each sample, and a straight line was fit to the data.

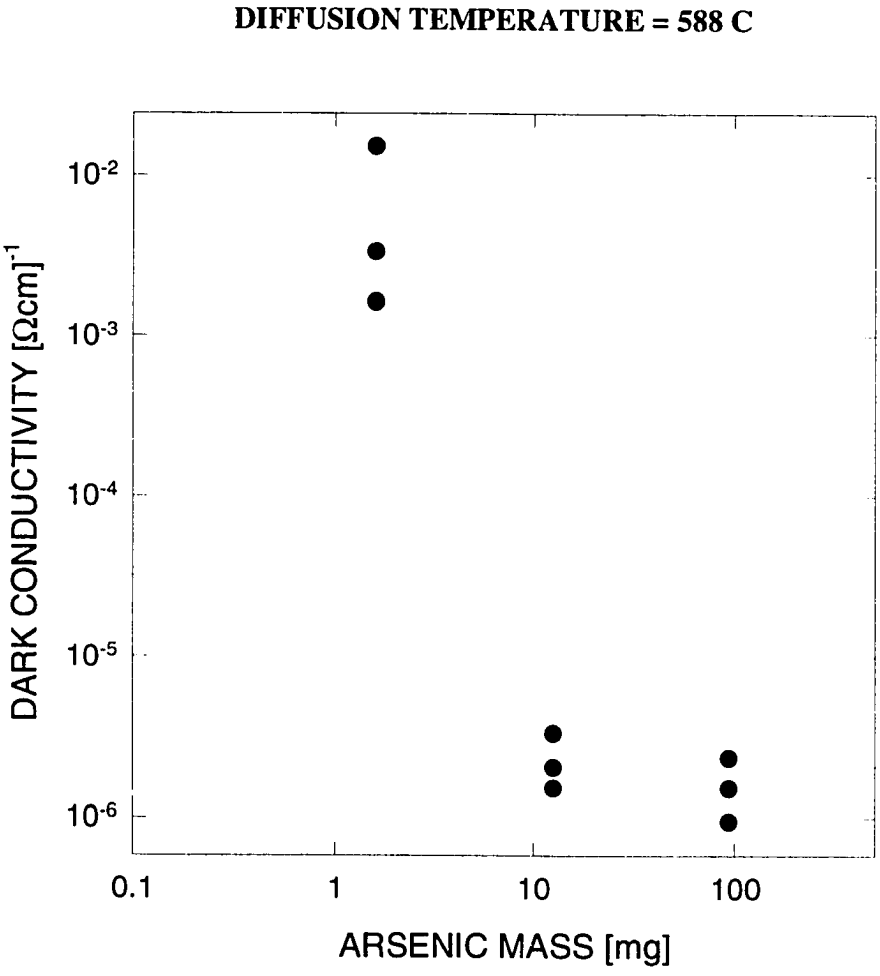

Figure 4.1.2. Conductivity for samples compensated at the same temperature, but with different arsenic background pressures.

The compensation curves for wafers 57 and 23 were developed using the same techniques as those used with the other wafers. Plotting the compensation curves for all of the wafers on the same graph shows the behavior of the compensation process as the temperature and silicon densities are elevated. Figure 4.1.3 demonstrates that compensation at higher silicon densities (higher temperatures) gives a comparably sharp compensation curve. In chapter 3, this behavior was attributed to the distribution of the copper atoms among the various deep copper acceptors. For example, if most of the copper forms Cu_B, then high copper densities (relative to silicon) may still produce a highly resistive semiconductor. This is because the Cu_B center is relatively deep (0.44 eV), whereas the Cu_A level is shallow (0.14 eV). Therefore, excess amounts of Cu_A will cause the sample to have a high conductivity.

Changing the arsenic mass in the ampoules with wafers 23 and 57 (higher silicon densities) had little effect on the outcome. Raising the arsenic pressure in the ampoule did not produce a sample with a lower conductivity as was shown for the lower silicon densities. This may be due to the enhancement of a deep donor level such as EL2, which has known concentrations near $1x10^{16}$ cm^{-3} and has been proposed to be associated with arsenic-related complexes. Arsenic vacancies and interstitials are believed to be associated with native defects such as EL2.[39] Also, one or both of the two dominant copper levels may be associated with the arsenic vacancies. This implies that limited control of the deep level configuration may be possible by changing the processing environment, such as with arsenic partial pressure in the ampoule. For samples with higher densities of silicon, the arsenic pressure did not affect the conductivity appreciably.

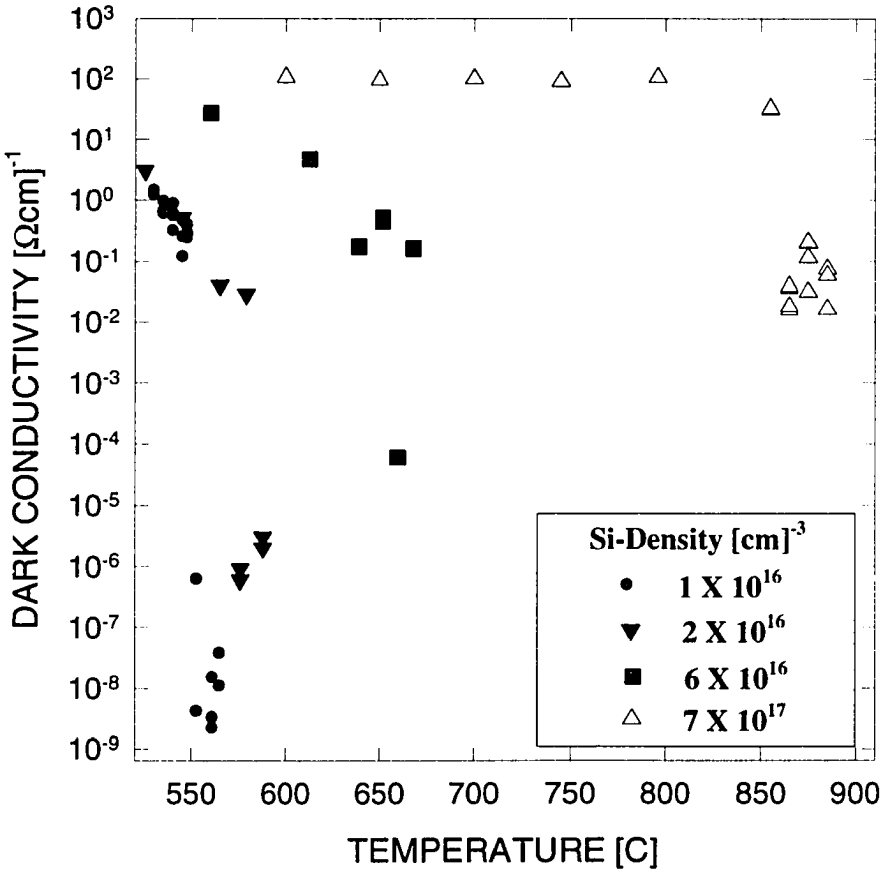

Figure 4.1.3. Compensation curves for wafers of four silicon doping densities.

4.2 Copper Solubility

The important information to be extracted from figure 4.1.3 is that the n-type GaAs was converted to p-type through the thermal annealing process, and that the approximate copper concentration can be found. The hypothesis is that a solid solubility limit is reached in time for a given temperature at which the maximum amount of copper has diffused into the crystal. At the temperature at which conversion to p-type is achieved (called the compensation point as before), the copper density is considered to be equal to the silicon density. This idea is supported by plotting the concentration versus the compensation point temperatures and comparing it with a copper-solubility curve. It should be noted that the silicon density is approximated by the free-electron density because the silicon donors are thermally ionized at room temperature. The temperature corresponding to the lowest measured conductivity for each wafer is plotted in figure 4.2.1 against copper-solubility measurements made by others. As shown in this figure, the data agrees with that given by Fuller and Whelan[15], and Hall and Racette[14]. A curve fit indicates an exponential relationship, which is also given by Fuller and Whelan.

$$N_{Cu} = 3.3x10^{23} e^{-1.3/kT} \qquad 4.1$$

where N is the density, and kT is in units of eV. This means that the compensation temperature can be predicted for a given silicon doping density assuming that copper is singly ionized in GaAs:Si:Cu. It should also be noted that these compensation experiments have been repeated for several different annealing times (2-24 hours) with similar results, which supports the idea of a copper solubility limit.

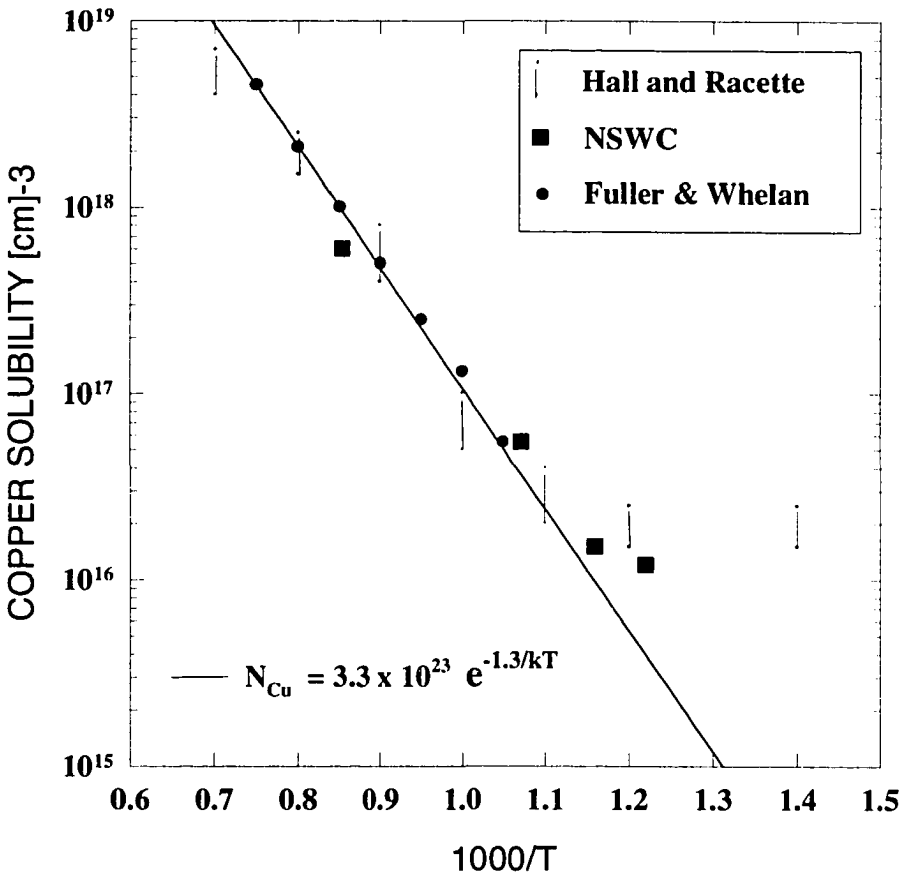

Figure 4.2.1. Copper solubility data obtained through compensation compared to data given using other techniques.

4.3 Comparison with Model

The data described in the previous sections can be interpreted using the model presented in chapter 2 (compensation model). The results of such a comparison are shown in figure 4.3.1. Using a model with two copper levels located 0.14, and 0.44 eV with respect to the valence band, and a silicon density of $1x10^{16}$ cm^{-3}, the model can be matched reasonably with the experimental data. In this figure it is also apparent that the linear temperature scale on the top axis compares favorably with the exponential copper density scale on the bottom axis. This verifies the exponential relationship found with a curve fit to the copper solubility data (figure 4.2.1). Also, samples prepared with various amounts of arsenic in the ampoule are shown to dramatically change the conductivity. Lower arsenic masses correspond to lower conductivities which implies that a shallow acceptor such as Cu_A is predominantly created under these conditions. Therefore, the model demonstrates the importance of the various deep levels which are known to exist in this material. Specifically, excess amounts of EL2 in the model reduced the post-compensation conductivity to values below those which can be achieved with copper acceptors alone (solid line in Figure 4.3.1). With increasing copper concentration, the low conductivity regions rise to values which are predicted using only copper acceptors and silicon donors. Also, a ratio of Cu_A to Cu_B densities that is much larger that unity can cause the low conductivity region of the curve to occur over a smaller temperature range (dashed line in Figure 4.3.1). The data and calculations demonstrate that a simple model gives insight into the nature of the compensation process for GaAs:Si:Cu with respect to the deep level configuration and processing parameters.

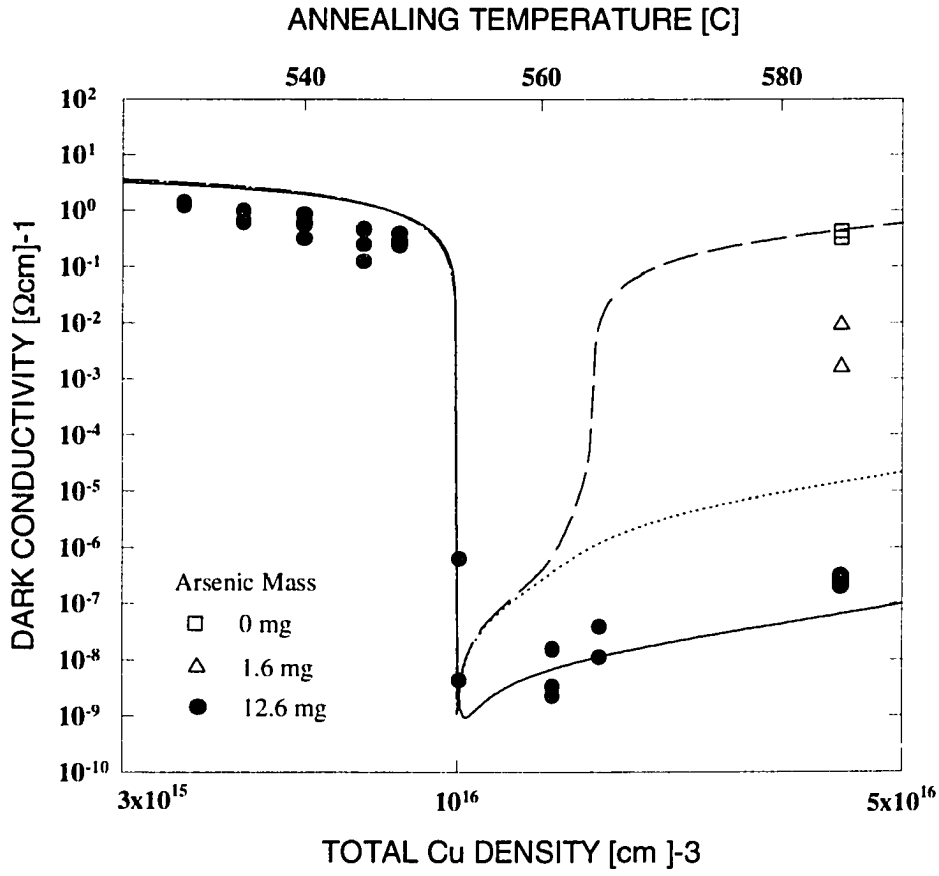

Figure 4.3.1. Compensation data compared to the model given in Chapter 2.

4.4 Compensation by Heat Treatment without Copper

Heat treatment of GaAs produces shallow and deep levels in concentrations that depend on the temperature and time of the anneal as well as the arsenic pressure in the ampoule.[23] In order to determine the effects of heat treatment on the gallium arsenide wafers, several samples were loaded into ampoules with various amounts of arsenic but without any copper. Three anneal times were used (10, 105, 3900 minutes), and three arsenic pressures (0, 115, 1137 Torr - As_2). The results show that compensation was achieved (conductivity $\approx 3x10^{-5}\ \Omega^{-1}cm^{-1}$) for the 1000 °C anneal at 1137 Torr arsenic pressure, and an anneal time of 105 minutes. Under otherwise identical conditions, low arsenic pressure (0 mg in ampoule) resulted in a wafer that was converted to relatively heavy p-type ($10^{17}\ cm^{-3}$). These results show that a shallow acceptor is formed upon heat treatment at 1000 °C. The concentration of this acceptor is controlled by varying the anneal time and the arsenic pressure in the ampoule. At the operating point that demonstrated compensation, it may be assumed that an acceptor was formed with a density of approximately $2x10^{16}\ cm^{-3}$, which is the amount required to compensate the silicon donors. It is not clear as to the exact origin of these shallow acceptors which may be due to impurities (Fe, O, Cu, etc.), silicon site-switching ($Si_{Ga} \rightarrow Si_{As}$), or native defects from Frenkel/Schottky disorder. Finally, samples that were previously compensated by the copper diffusion technique, simply were inundated with additional shallow acceptors during these heat-treatment experiments, and therefore were rendered highly conductive thus losing the low conductivity properties obtained through copper compensation.

The surfaces of the samples subjected to the heat treatments were degraded in varying degrees depending on the time and arsenic pressures. Figure 4.4.1 shows the surface of the samples for the various conditions. It is apparent that for low arsenic pressures, the sample surface was better preserved after an anneal at 1000 °C (top left in figure 4.4.1). Higher arsenic pressures caused more damage to the surface (top right picture in figure 4.4.1). In fact, at 1100 Torr arsenic, and 3900 minute anneal time, the surface pit depths peaked at about 0.02 cm which represents a substantial damage to the wafer (bottom left).

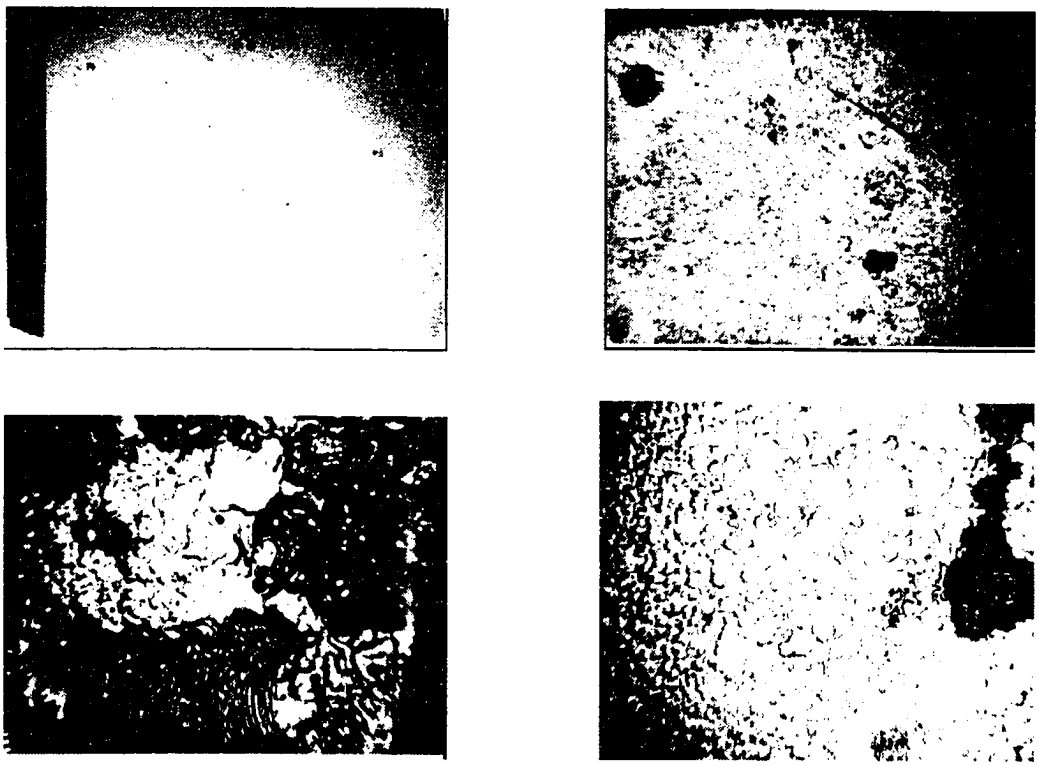

Figure 4.4.1. Surfaces of samples annealed for one hour with (clockwise from top left) 0, 1, 10, 100 mg arsenic in the ampoule during diffusion.

CHAPTER 5

CHARACTERIZATION

The gallium arsenide wafers prepared using the techniques described in chapters three and four are to be analyzed using several different characterization techniques. The purpose of the characterization experiments is to understand the electronic and physical properties of copper in gallium arsenide. Of particular interest is the behavior of the material under illumination from the two laser pulses used to excite the BOSS devices (one and two micron wavelength). Hall measurements are used to obtain the sample conductivity over a wide range of temperatures in order to extract deep level information and to generate the compensation curves. In addition to the electronic characterization, the physical nature of the copper diffusion is important. Therefore, Glow-Discharge Mass Spectroscopy and Secondary-Ion Mass Spectroscopy techniques are used to measure the depth and surface profiles of the copper atoms in the copper-doped gallium arsenide samples.

5.1 Hall Measurements

The most common characterization technique used with semiconductors is the Hall Effect technique.[40] This method is a four-point probe analysis which eliminates most problems with contact resistance. The conductivity is extracted initially, and then the

mobility is measured using the proper magnetic field alignment. Van der Pauw developed a technique to obtain the resistivity of a flat arbitrarily shaped, continuous semiconductor using a four-point-probe measurement.[40] In Hall, measurements a magnetic field is applied perpendicular to current flow to deflect the current such that a voltage is measured transverse to the current flow. This voltage is used to determine the mobility, and therefore the carrier concentration is calculated using the mobility and conductivity values.

The technique employed in this work involves a system which is capable of measuring the Hall effect in semiconductors with resistivities between 10^{-2} and 10^{10} Ωcm in the temperature range of 100 to 500 K. A block-diagram for this system is shown in figure 5.1.1. The sample is mounted in a cryostat on a small piece of alumina which is attached to a flat copper strip (1/16" thick) with thermal paste. The copper strip is attached to a cold finger with two screws, and therefore the temperature at the cold finger should be similar to that at the end of the copper strip provided a vacuum is maintained in the chamber (10 mTorr). Four wires are applied to the sample contacts as described in chapter 3 with silver epoxy. Each wire is fed through the cryostat flange and into triaxial cables. The use of triaxial cables is necessary in order to test very high resistance samples. Cable charging times are almost eliminated using guarding techniques with triaxial cables instead of unguarded coaxial cables.

The electrical measurements are made with a series of Keithley instruments. The voltage is measured using a Keithly 617 electrometer, and the current is measured using a Keithley pico-ammeter. The current is supplied using a constant current source. In order to buffer the signals, a Keithley 7065 Hall effect card is used which contains four

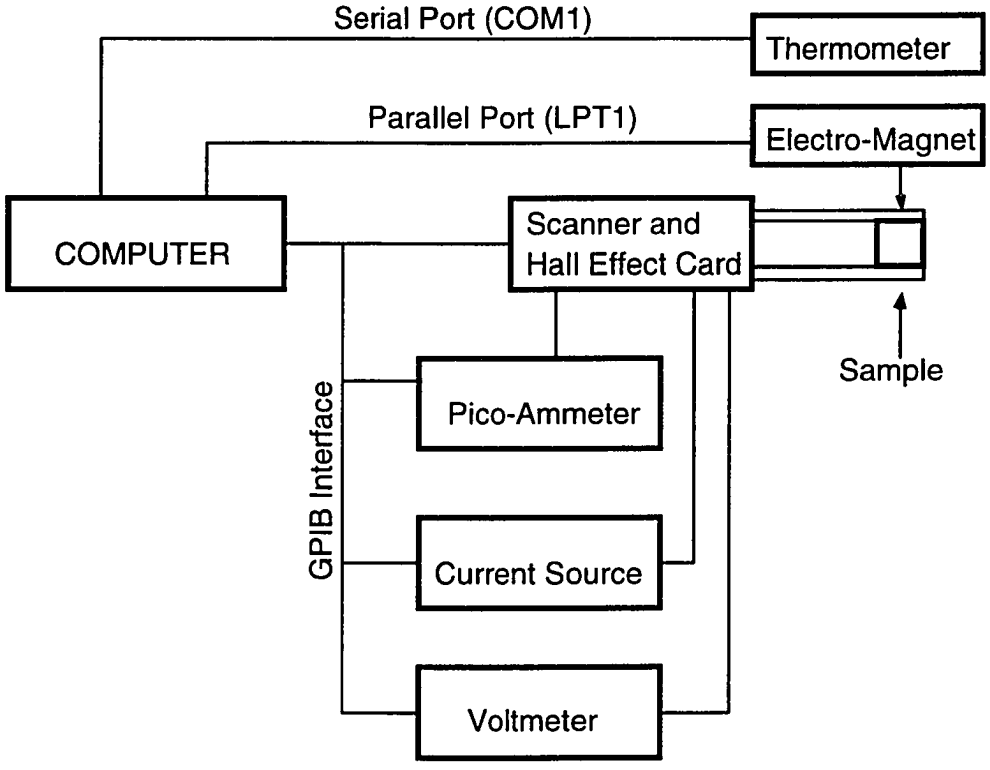

Figure 5.1.1. Hall-system schematic.

electrometer buffers. This is necessary because this technique requires differential measurements to be made. In order to switch the connections as required by the Van der Pauw and Hall measurements, the Keithley 7001 scanner is used. This instrument contains the 7065 Hall effect card, and allows the different instruments to be switched to the desired sample contacts. The sample is mounted in the cryostat which is inserted between the poles of an electromagnet which supplies the 3000 G magnetic field. Since the cryostat is made of stainless steel, the magnetic field is not significantly disturbed by the cryostat walls. All of the Keithley instruments described above are linked together by GPIB (General Purpose Interface Board), the electromagnet is controlled using a set of relays linked through a parallel port, and the Omega thermometer is controlled through a serial port. All of these instruments are connected by a computer program which automates the entire system (given in Appendix B). The purpose of the program is to take measurements at prescribed temperature intervals. Data averaging and rapid acquisition are required in order to obtain a large data sample space. Also, the program performs the calculations for the sample conductivity, mobility, and carrier concentration for each temperature. Upon cooling the system down using liquid nitrogen, the program automatically operates as the temperature naturally rises. When the temperature changes by about 1 K, the conductivity is measured followed by the Hall effect measurements which require the magnetic field to be reversed. This is done by simply reversing the current in the coils of the electromagnet. Measurements of the magnetic field under reverse current have shown that the magnitude of the field is not changed significantly by hysteresis effects. When the temperature of the system rises near 300 K, a heater is

applied to the cold finger in order to heat the sample beyond room temperature. Using this technique, Hall measurements can be performed for temperatures in the range of 100 - 500 K.

The measurements of interest here involve the compensated GaAs samples described in the previous chapters. In order to simply determine the level of compensation in the samples, Hall measurements were made to extract the sample conductivity, carrier type and concentration. The carrier type is important because the compensation point is characterized by a change from n-type to p-type. During the compensation experiments described in chapter 4, the Hall measurements were made to generate the compensation curves and to determine carrier type which allows the compensation point to be experimentally isolated. All of these initial characterization experiments are performed at the same temperature (300 K).

Measurements of the temperature profiles for the doped material is also of interest for the extraction of deep level information.[41-43] Copper-doped samples have been tested using this technique. Two samples used here were annealed at 900 °C (sample #57-08) and 588 °C (sample #69-03) in the presence of copper and arsenic. The effects temperature and varying the arsenic partial pressure are examined in this series of experiments. The idea is to determine the difference between the samples of two annealing temperatures. Also, a gallium arsenide sample heat treated with no copper present during the anneal has been tested. The purpose of this set of samples is to determine show the dominant copper levels formed with the two annealing temperatures and two arsenic pressures, and to determine the effects of heat treatment alone.

The first sample tested (sample #57-08) was annealed at 900 °C with 1 mg of arsenic present in the ampoule. Figure 5.1.2 shows the hole concentration as a function of temperature which was obtained from the measurements. Equation 2.38 can be simplified for one dominant energy level and fit to the data, and a similar treatment has been shown by Blakemore[44,25],

$$\frac{p(N_D + p)}{N_A - N_D - p} = \frac{N_v}{4} e^{\frac{-E_A}{kT}} \qquad 5.1$$

where the symbols have the same meaning as described in chapter 2. An approximate value for the activation energy can be obtained from the plot of hole-density versus 1000/T. From figure 5.1.2, an activation energy of 0.1439 was measured using a fit to equation 5.1. This value compares favorably to that of the Cu_A level. The curve obtained for sample #57-09 (which was annealed at 900 °C with 100 mg of arsenic present in the ampoule) gives a best fit which also shows a dominant Cu_A level. In this case, however, it appears that another level is contributing to the curve. The effect is small enough that the value for the activation energy is not completely accurate, but a level around 0.6 eV was measured. This could be the Cu_B level, but it must be stressed that the accuracy of this number should be questioned. The main point to be made here is that more than one level contributes to the curve. Therefore, the observance of an additional level may be attributed to excess arsenic in the ampoule during the anneal.

Sample #88-02 was tested to show the levels formed during the lower temperature anneals. The results of the Hall measurements are shown in figure 5.1.3 along with the results obtained from sample #57-08 over the same temperature range. The curve for 69-

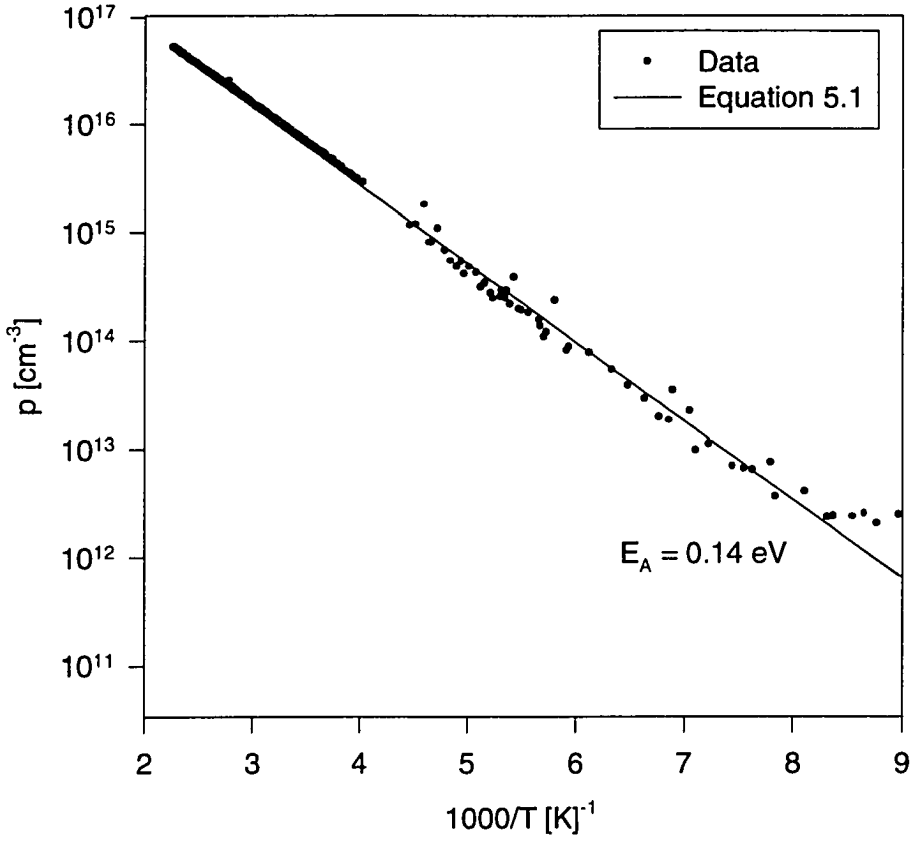

Figure 5.1.2. Hall data for a sample that was annealed at 900 °C.

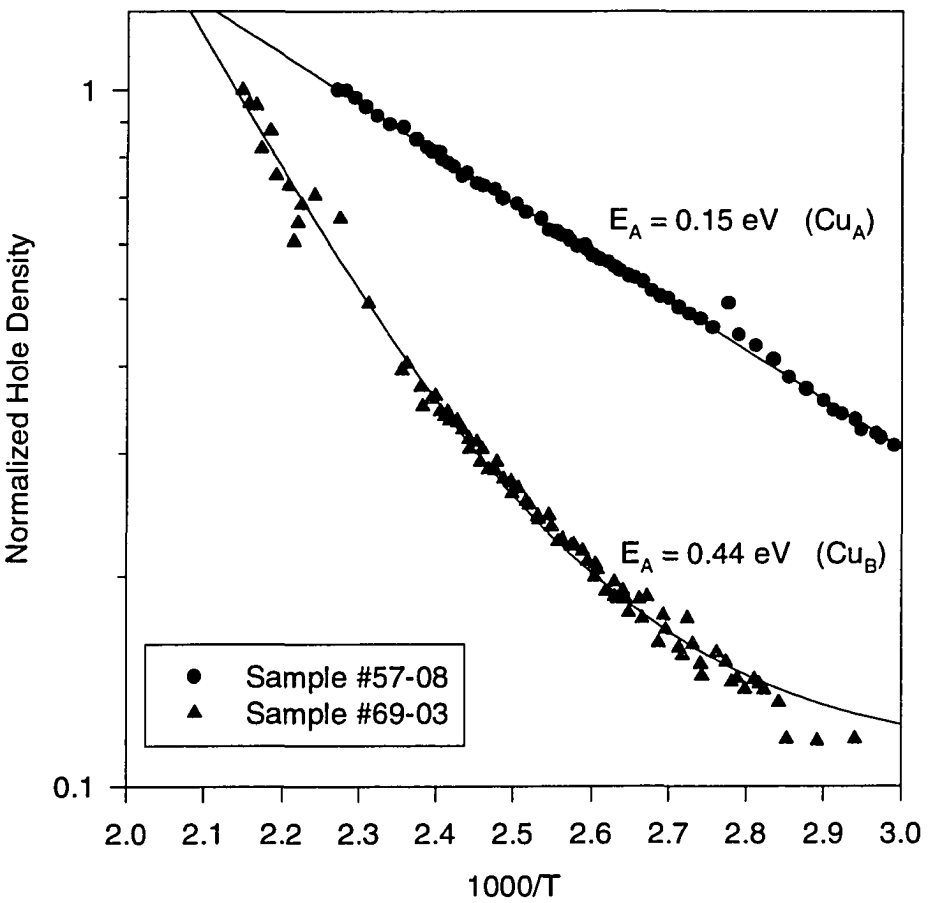

Figure 5.1.3. Comparison of Hall data for two copper-doped samples.

03 shows that the dominant level formed has an activation energy of 0.44 eV which corresponds to the Cu_B level. Figure 5.1.3 demonstrates the difference between samples annealed at these two temperatures. As hypothesized in Chapter 4, it is apparent that the dominant level is Cu_A at higher temperatures and Cu_B at lower temperatures. This data confirms the hypothesis that compensation at higher temperature must involve Cu_A rather than Cu_B under these processing conditions.

Similarly, a sample which was annealed at 1000 °C for one hour with no copper or arsenic present in the ampoule was tested. This sample was found to be p-type, and fitting equation 2.38 to the data shows that several rather shallow levels must be present in order to model the data. This means that the high temperature anneals generate a dominant shallow acceptor along with several other less prominent levels under these experimental conditions. This is important because the data demonstrates that compensation is possible using the creation and/or enhancement of defect levels in the bulk of the crystal.

5.2 Infrared Photoconductivity

As described in chapter 2, it is very important to address the issues concerning the absorption of two infrared laser sources in copper-doped gallium arsenide which are used to excite and quench the photoconductivity. The goal here is to use the samples developed in the compensation experiments (chapter 4) to determine how the processing changed the occupancy of the deep levels. First, the maximum steady-state photoconducitvity is measured for the different processing parameters in order to determine the extent to which the copper level, Cu_B, was changed. Specifically, it is of

interest to try to enhance the photoconductivity in order dissipate less power in the semiconductor during the on-state.

The on-state conductivity measurements were made using the circuit shown in figure 5.2.1. A capacitor was charged and applied to the sample which was in series with a 1 Ω current-viewing resistor (CVR). The applied laser pulse was from a home-made Nd:YAG laser system which delivered up to 20 mJ of energy in a Gaussian, 20 ns (FWHM) pulse. The electrical measurements were made with a Lecroy 7200 digital oscilloscope. Upon application of the laser pulse to the sample, the current flows to the load (CVR), and measurements are made for various laser intensities. The laser intensity is changed by using a series of calibrated neutral density filters. A typical sample response to the 1 μm laser pulse in the circuit of figure 5.2.1 is shown if figure 5.2.2. In order to calculate the steady on-state conductivity, the current at 150 ns after the peak is used with applied voltage and sample geometry. This ensures that the laser pulse has no effect on the current, and provides a conservative measurement of the on-state conductivity.

The samples used in these experiments have three different doping densities. The silicon densities are 1, 2, $5x10^{16}$ cm^{-3}, which indicates that a similar amount of copper was doped into the samples during the compensation process as described in chapter 4. The prediction of equation 2.21 implies that the maximum steady on-state conductivity is increased with increasing copper density. Figure 5.2.3 shows the effect of changing copper density on the on-state conductivity. Also, changing the amount of arsenic in the ampoule during the diffusion process changes the on-state conductivity slightly. These factors demonstrate that limited control of the on-state conductivity is achieved by

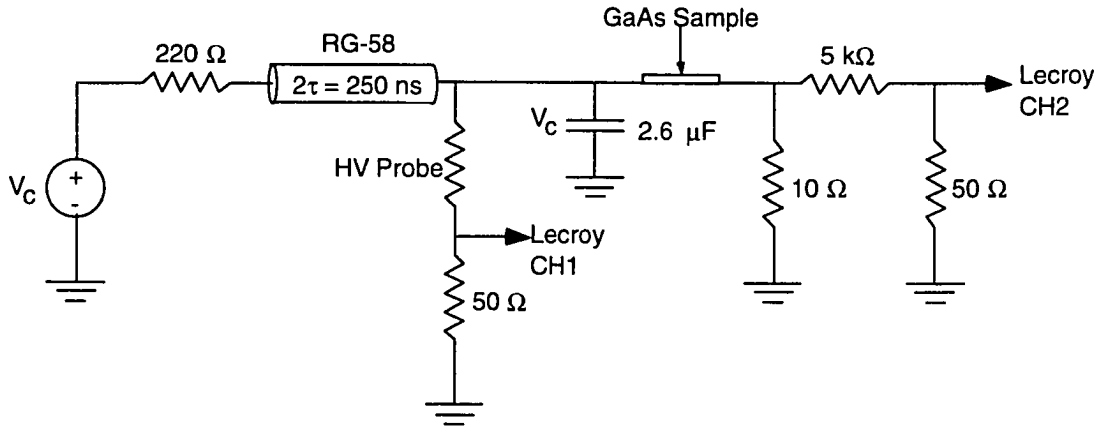

Figure 5.2.1. Circuit used in the on-state photoconductivity experiments.

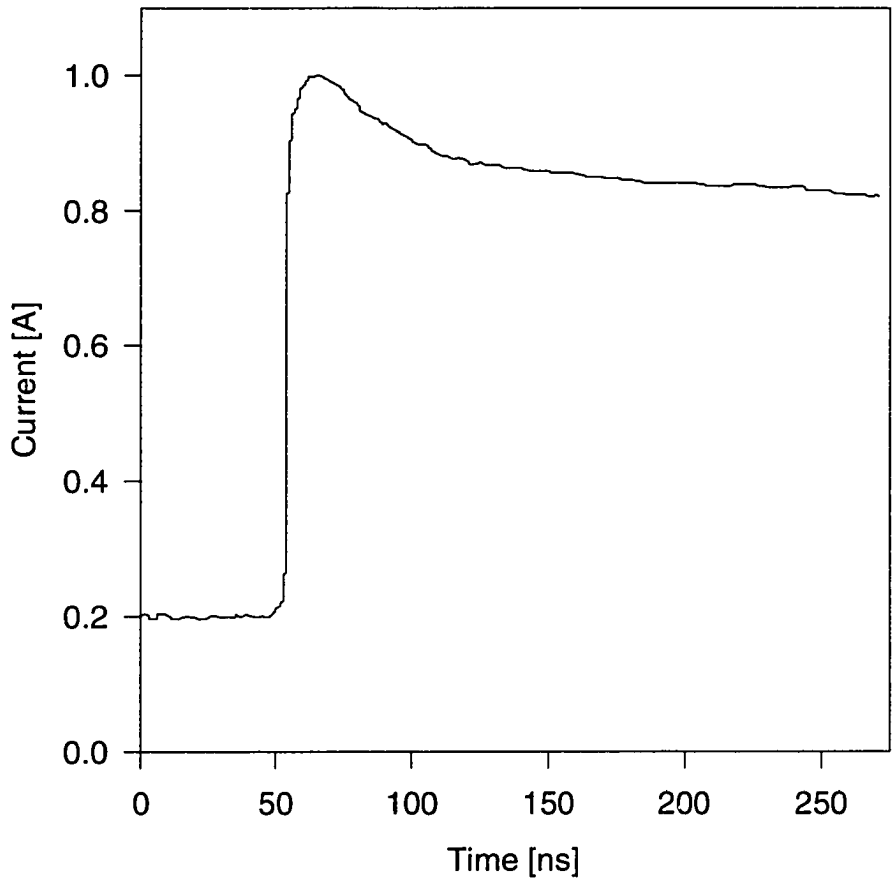

Figure 5.2.2. Typical response of copper-doped gallium arsenide to the 20 ns FWHM, 1.06 μm wavelength laser pulse.

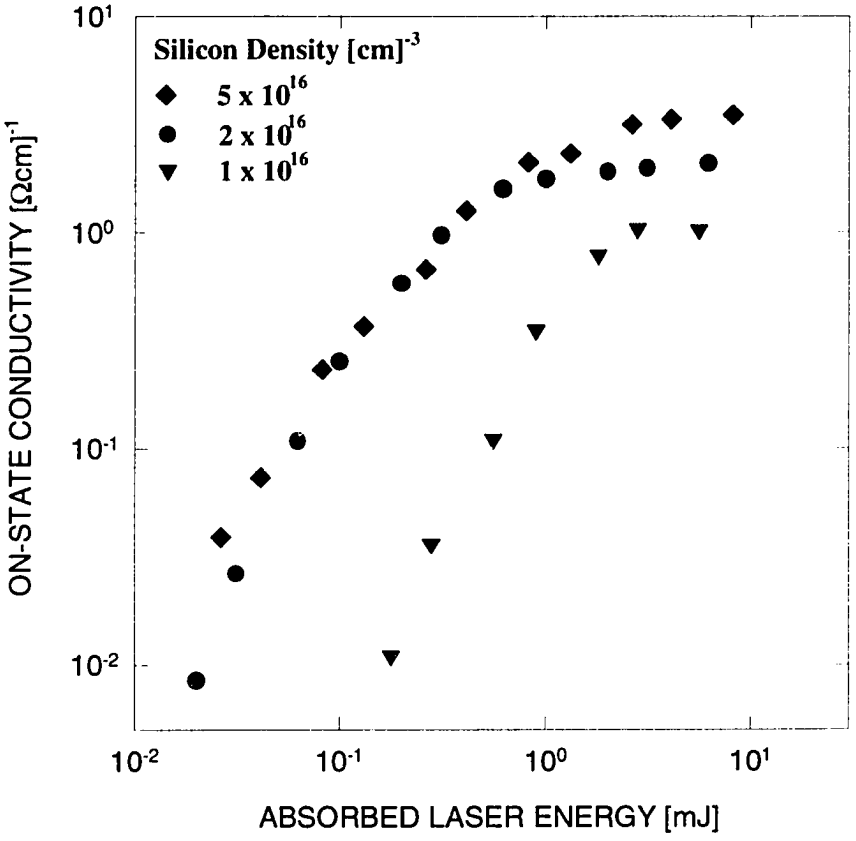

Figure 5.2.3. Responses of various samples to the 1.06 μm wavelength laser pulse for several absorbed energies.

varying the processing parameters. For the highest doping density, the on-state conductivity saturated at approximately 4 $(\Omega cm)^{-1}$, whereas the lower density material saturated at about 1 $(\Omega cm)^{-1}$. Excess arsenic pressures during diffusion decreased the maximum conductivity achieved, which may be due to the dependence of the Cu_B level on arsenic vacancies and/or interstitials. The results are significant because they show that the device can be improved by increasing the deep center density in the switch material through semiconductor processing techniques.

Excitation of the samples with a fast laser source at 2.1 μm wavelength shows the hole trapping kinetics. A new circuit was built to accommodate switch excitation with a 140 ps (FWHM), 2.1 μm wavelength laser pulse, and therefore the circuit bandwidth was required to be approximately 5 GHz. The system shown in figure 5.2.4 was assembled with a microstrip line used for charge storage and delay line. The strip line and SMA cable were designed to deliver a 20 ns voltage pulse to the sample (about 30 V). A delay line was built into the system so that upon excitation, any reflections occurring at the transition from strip line to cable will occur after the current has decayed sufficiently. The fall time of the current trace is of great interest because after the laser pulse ends, hole trapping determines the fall time of the current pulse (provided the hole trapping is slower than the laser pulse).

The purpose of this experiment is to measure the hole trapping times for the Cu_B, Cu_A, and Cu_C levels, and determine the effects of changing the doping densities. It should be noted that n-type contacts were applied to the samples in accordance with the discussion in chapter 3, and these experiments are designed to measure a p-type current

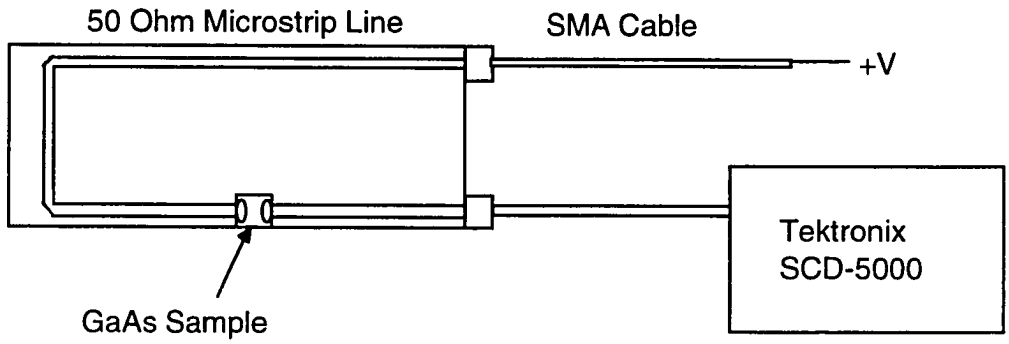

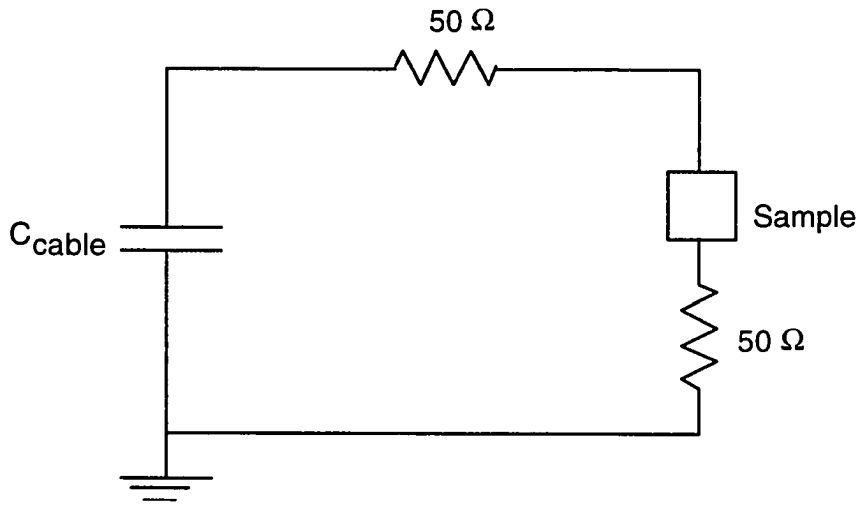

Figure 5.2.4. Circuit used for the fast (140 ps), 2.1μm wavelength laser excitation.

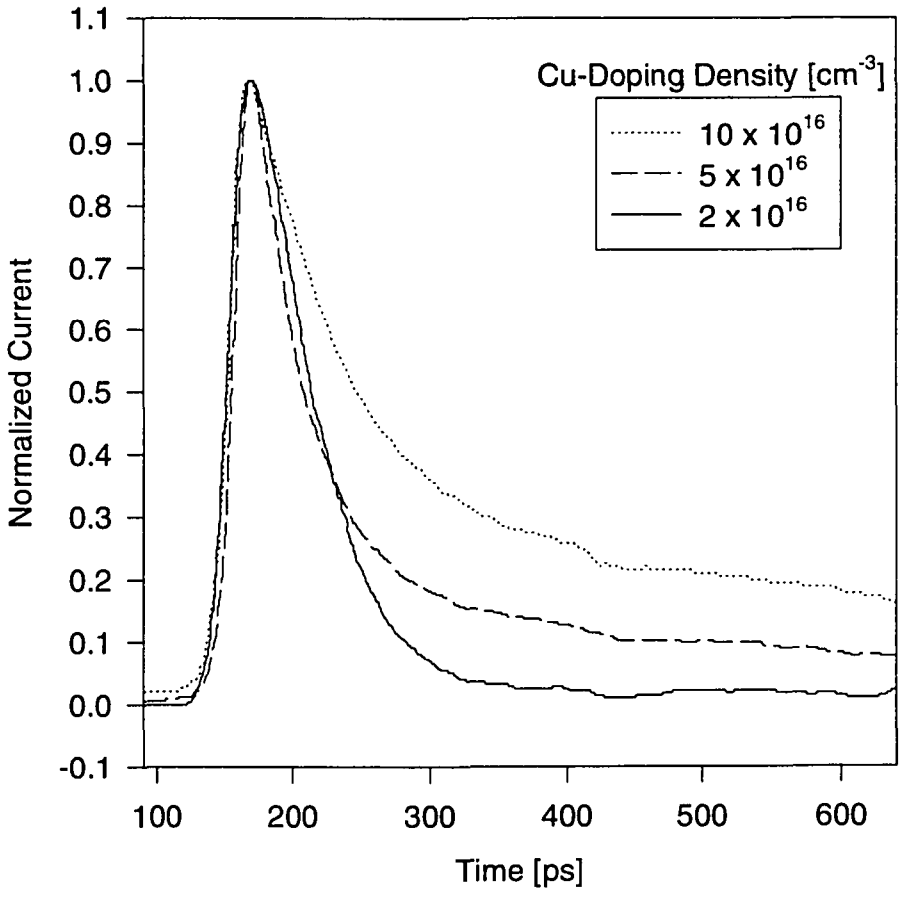

Figure 5.2.5. Response of the samples to the 2.1 μm wavelength laser pulse.

flow. This might be a problem on longer time scales (many ns), but the displacement current at the n-p anode has a sufficiently long time constant to allow these contact effects to be ignored. The experiments carried out involved the same three samples as used for the on-state conductivity measurements. Figure 5.2.5 shows the effect on the hole trapping time of changing the doping density. The lowest doping density sample response effectively follows the temporal characteristics of the laser pulse. The total hole trapping time appears to increase with increasing doping density, and this is consistent with the analytical results shown in chapter 2. Therefore, it has been shown that the hole trapping time can be manipulated by changing processing parameters such as copper doping density. This is important when considering the design of an optically activated switch such as the BOSS device which relies on tailoring the hole trapping in order to enhance optical quenching effects.

5.3 Glow Discharge and Secondary Ion Mass Spectroscopy (GDMS, SIMS)

In order to determine the physical nature of the copper in GaAs with respect to the processing procedures, it is necessary to employ physical characterization techniques such as GDMS and SIMS[7]. These techniques rely on removing layers from the surface of the wafer and discriminating based on atomic mass. The SIMS technique sputters atoms from the surface creating some secondary ions. The ion yield is a calibrated, known constant for a given material. This technique is quite adequate for surface analysis in the detection of all elements in the Periodic Table for the parts-per-billion (ppb) to parts-per-million (ppm) range. Low sputter rates cause the depth resolution to be less than 100 Å with a

sputtered area as small as 2 μm x 2 μm. The GDMS system involves a glow discharge which sputters material away at a much higher rate, thus depth profiling may be accomplished. The sensitivity is similar to SIMS, but GDMS is semi-quantitative and relies on the use of calibration numbers.

The set of numbers used for calibration must be well known in order to determine concentrations accurately. The SIMS technique uses standards which were developed by ion implantation techniques. These ion-implantation standards are fairly well known and readily available. The GDMS method uses a set of Relative-Sensitivity-Factors (RSF's) which are not quite as well known. It is important to note that the information that is desired here is the relative concentrations across the surface and with depth. Therefore, the actual numbers are not critical to the outcome of the experiment. It is important, however, to calibrate the systems to deliver numbers as accurately as possible.

Non-uniformities in the compensated GaAs material may be due to non-uniform copper doping or non-uniform silicon doping. Therefore, it is important to characterize the wafer as delivered by the manufacturer. Using the SIMS technique it was found that across the surface of the wafer, the silicon density varied by approximately 10%. Near the edges of the wafer (within two millimeters), the silicon concentration dropped by about a factor of two. Also, GDMS measurements were made for a depth profile of the silicon density which show that there is 10% depth uniformity as well. These measurements were made with both wafers 57 and 88 (see Table 4.1), which correspond to the lowest and highest silicon densities respectively (2 and 7 $x10^{16}$ cm^{-3}).

Next, the copper-doped samples described in chapter 4 were tested using the GDMS and SIMS techniques. Again, wafers 57 and 88 were used in these experiments. Wafer 57 was doped with copper at a diffusion temperature of 825 °C, and 88 was diffused at about 570 °C. Using the results of the compensation experiments, the copper density for wafer 57 is approximately $8x10^{17}$ cm^{-3} and $4x10^{16}$ cm^{-3} for 88. Using the SIMS technique, the sensitivity is rather poor for copper detection but there is definite demonstration of significant non-uniformity across the surfaces of both samples. The GDMS results were far more quantitative than those of SIMS. The copper concentration was shown to vary from 10 ppm (parts-per-million) to 130 ppm for wafer 57, which corresponds to about $5x10^{17}$ cm^{-3} to $6x10^{18}$ cm^{-3}. The concentrations varied from 1 to 6 ppm for wafer 88 ($5x10^{16}$ to $3x10^{17}$ cm^{-3}). At the same time, the silicon density appeared to be uniform over the same depth for both samples which rules out any instrumental effects causing the copper depth profile. It is also interesting to note that the highest copper concentrations occurred approximately half-way through the sample. In other words, as material was sputtered, the concentration increased until the center of the sample was reached and decreased from the center to the opposite side. This may be due to the diffusion of copper from both sides of the sample meeting in the center. These experiments have demonstrated that the copper diffusion is non-uniform with respect to depth and surface position, and the measured concentrations are consistent with the compensation experiments and solubility measurements.

CHAPTER 6

DISCUSSION AND CONCLUSIONS

The purpose of this work is to demonstrate the controlled compensation of gallium arsenide which is initially doped with several different silicon doping densities, and to generate characterization data which provides insight into the physical and electronic nature of the dopants. The major concern here has been compensation by diffusion of copper acceptors because of the technological importance of copper-doped gallium arsenide in photoconductive switching. Specifically, the correlation between annealing temperature and copper acceptor formation was shown. Also, compensation was demonstrated using heat treatment with varying arsenic partial pressures in order to introduce defect acceptor levels (unrelated to copper) which compensate the donors.

6.1 Processing and Compensation

The preparation of the samples involved the thermal diffusion of copper into gallium arsenide by heat treatment in the presence of copper and arsenic vapor. The goal is to correlate the compensation and electronic effects with both copper density and arsenic vapor pressure. The compensation curves were developed for several different doping densities, and it was shown that controlled compensation was achieved for the lower doping densities more easily in comparison to the higher densities. The reasons for this difference originate with the elevated diffusion temperatures required to obtain high

doping densities. This indicates that the distribution of copper among the three known copper-related deep levels is a function of temperature. The results of the compensation are shown in Table 6.1. It appears from the data that at higher temperatures, the shallow copper level becomes dominant due to the decrease in conductivity. This is a logical conclusion given that the curves shown in chapter 4 for the higher doping densities demonstrate behavior consistent with the compensation of a shallow donor by the addition of a shallow acceptor.

Attempts to alter the distribution of copper acceptors through the introduction of arsenic related defects were carried out by varying the arsenic partial pressure in the diffusion environment. The results showed that decreasing the arsenic partial pressure caused a corresponding increase in the shallow acceptor density. Assuming that the shallow acceptor is copper related, then it can be concluded that Cu_A is enhanced by the introduction of arsenic-rated defects such as vacancies. The higher density material (higher diffusion temperatures) did not show a reduction in the shallow acceptor density with increasing arsenic mass in the ampoule over the range 0-100 mg. This is most probably due to insufficient arsenic pressure in the ampoule. Higher arsenic pressures must be used at the elevated temperatures in order to see an effect.

Some of the potential problems with higher temperature diffusion were outlined in chapter 3, and were related to non-uniform boundary conditions at the gallium arsenide surface. The first solution to aid in the uniformity issue was to use a vapor-phase source of copper instead of copper plating on the surface. Past experiments with copper plating cause non-uniform boundary conditions because of copper pealing from the surface due to the surface tension created in the high temperature diffusion environment. The vapor-

Table 6.1. Summary of the compensation data.

Wafer #	Silicon Density $[cm]^{-3}$	Compensation Temperature [C]	Conductivity at Compensation $[\Omega cm]^{-1}$
88-87	$1x10^{16}$	553	$2x10^{-9}$
88-68	$2x10^{16}$	587	$7x10^{-7}$
23-22	$6x10^{16}$	650	$8x10^{-5}$
57-23	$7x10^{17}$	855	$1x10^{-2}$

phase diffusion is considered to be a much more uniform method of introducing copper and arsenic to the surface of the sample during diffusion. This is supported by photographs taken after diffusion using both plating and vapor-phase techniques.

Other sources of non-uniformities are probably due to the relatively unclean environment in which the diffusion is performed. For example, the solid sources of copper, arsenic, and gallium arsenide are all exposed to the atmosphere for extended periods of time before they are contained under vacuum (several hours). Therefore, natural sources of contamination builds on the surfaces. This contamination may react with the arsenic to form precipitates on the surface at random locations. One example is a tan-colored, circular-shaped discoloration on the surface of a sample after diffusion that encompassed approximately 10% of the surface area. Cleaving the sample along the discoloration revealed that the pattern spanned the entire depth of the sample going from one side to the other. This demonstrates that the diffusion environment used in this work is far from ideal. There is, however, enough ability to control some important aspects of the diffusion such that meaningful results are obtained.

The development of devices based on copper-doped gallium arsenide must involve more advanced processing techniques. This becomes a problem because semiconductor processing facilities will not introduce copper into their expensive systems due to contamination. Copper is a very undesirable contaminant in the gallium arsenide industry, and therefore processing copper-doped GaAs will not be performed by standard sources. A strong market-potential must be developed through device design work such as shown

here in order to generate the funds required to elevate the sophistication of the present processing methods.

6.2 Characterization

Three methods of characterization were used in this work to determine the effects of changing copper density on the distribution of the copper acceptors among the known copper-related defects. Also, the physical distribution of the copper was measured using mass spectroscopy techniques in order to determine uniformity in the diffusion process. First, the development of the compensation curves gave information about the possible formation of the various copper levels. The analytical model presented in chapter 2 demonstrated that excess amounts of Cu_A are probably formed during the higher temperature anneals. Temperature-Dependent Hall effect (TDH) measurements were performed to quantify this presumption, and to provide other important information such as temperature-dependence of the mobility. Finally, photoconductivity measurements were made using infrared lasers to provide additional verification of the results and to demonstrate the feasibility of a fast (100 ps) photoconductive switch.

Temperature-Dependent Hall-Effect (TDH) Measurements

The Hall effect measurements have been used to determine the nature of the copper in gallium arsenide under various processing conditions. The temperature-dependent Hall effect technique was used to study the levels formed through high and low temperature anneals. An automated system was designed and built to perform the TDH

measurements over a wide temperature range (100-500 K). This system can take measurements on samples with resistivities in the range of 10^{-1}-10^{12} Ωcm. The purpose of the TDH measurements was to find the energy levels associated with copper impurities such that a relationship can be found with annealing temperature. Of particular interest was the copper levels formed in gallium arsenide of different doping densities (ie. annealing temperatures), and the levels formed through anneals without copper. Measurements were made on compensated samples with different copper densities as well as heat treated samples (no copper).

Based on the Hall-data for the copper-doped samples, it was evident that the Cu_A level becomes dominant at the higher annealing temperatures (900 °C), whereas the Cu_B level is dominant at the lower temperatures. This is consistent with the results of the compensation experiments which showed that at the higher doping densities (i.e. temperatures), the compensation curve agreed with the model for the case where Cu_A was dominant. The data also showed that samples annealed with no arsenic in the ampoule had significant Cu_A signatures. These results are summarized by showing the levels found in the various samples (Table 6.2).

Photoconductive Effects

The photoconductive switch described in this work relies on the two effects of turn-on and turn-off using two different laser wavelengths. The limitations of any switch involve power handling and speed. An ideal switch operates with zero on-state resistance, and it can be turned on instantaneously. Therefore, it is of great interest to study the

Table 6.2. Hall-effect measurement results

Wafer #	Annealing Temperature [C]	Dominant Activation Energy [eV]	Approximate Density $[cm]^{-3}$
88-87	565	0.44 (Cu_B)	$1x10^{16}$
88-68	588	0.44 (Cu_B)	$2x10^{16}$
23-22	675	0.15 (Cu_A)	$7x10^{16}$
57-23	900	0.14 (Cu_A)	$9x10^{17}$

conductivity of the switch during the on-state, and determine the minimum rise and fall times. Also, important material parameters can be obtained through such a study. In this work, the on-state conductivity and hole trapping times were measured as functions of the copper density. It was shown in chapter 2 that an increase of the Cu_B density results in a nearly linear increase in the maximum on-state conductivity using a laser excitation at a 1.1 μm wavelength. This means that measuring the saturation of the on-state conductivity provides a method of measuring the Cu_B density. It was shown that the Cu_B density does not increase linearly with the total copper density as predicted in Chapter 2. Therefore, it is concluded that copper centers other than Cu_B are formed preferentially as the diffusion temperature is raised. Again, this data is consistent with the results of the compensation and Hall-effect data. This is not a surprise given that the interaction between copper and arsenic-related defects form the copper acceptor levels, and this interaction is not a linear function of temperature. Instead of the expected factor of six improvement in the on-state conductivity, a more modest factor of four was achieved. This means that the Cu_B density was increased by approximately a factor of four through the higher temperature anneals. This data supports the Hall-effect measurements shown in Table 6.2 by demonstrating that the ratio of Cu_A to Cu_B densities (N_{CuA}/N_{CuB}) increases as the diffusion temperature is elevated.

Next, the hole capture times were measured using a fast (140 ps FWHM) 2.1 μm wavelength laser source. As described in chapter 2, this source causes excitation of holes from the copper levels to result in a photocurrent which can be easily measured. Three copper doping densities were studied, and the results show that the hole trapping times

increased with increasing doping density. Also, at least three modes are involved in the decay, which is consistent with two dominant copper acceptors (and a DC mode). It is important to note that the hole trapping times provide a limitation to the switching speeds that may be achieved by the photoconductive switch, and therefore it is concluded that switching times in the 140 ps time scale are possible provided that there is a direct or indirect recombination channel (band-band) that has a similar time constant. The fast hole capture at Cu_B is a benefit to the on-state because the conduction electrons are not lost to recombination. On the other hand, fast hole capture is a detriment to the turn-of effect because the recombination provide conductivity quench. It should be noted that the preferential formation of Cu_A causes an increase in the hole trapping time which is a detriment to fast infrared quenching. The optical effects demonstrated in this work have shown that the material can be optimized by adjusting processing parameters such that the photoconductive properties are tailored.

Physical Characterization

Secondary Ion Mass Spectroscopy (SIMS) and Glow Discharge Mass Spectroscopy (GDMS) were used to identify the physical distribution of the copper in the gallium arsenide crystal upon thermal diffusion. Using the SIMS technique to determine the uniformity across the surface, the copper density was shown to vary across the surface of the 1 cm square sample by as much as a factor of two. The sensitivity of the SIMS technique to copper was relatively poor, however, and therefore the results are somewhat qualitative. The GDMS results were more quantitative due to better calibration, and the

relative density was measured through the thickness of the samples. It was found that the copper concentration varied by as much as a factor of six across the depth of the sample with the highest density in the center of the sample. This could be due to diffusion of copper from both sides. Measurements of the conductivity of the samples after repeated polishing demonstrated that the conductivity increased with increasing depth which is consistent with the findings of the GDMS experiments. Therefore, the argument can be made that if the conductivity increases with depth, then the measured copper density is no longer consistent with solubility measurements as described in chapter 4 where uniformity of copper distribution was assumed. The error in the solubility measurements, however, are such that any inconsistencies can be explained. The solubility was measured not to define the copper concentration, but it was simply used as an indication of the temperature range for a desired copper density. Since the relationship between copper density and annealing temperature is exponential, it is useful to know that in order to get $1x10^{16}$ cm^{-3} Cu in the sample the annealing temperature must be between 550° C and 580 °C, for example. A full explanation for the relationship between conductivity depth profile and physical copper density depth requires measurements of both the total Cu-density distribution and the distribution of Cu in the various deep states.

6.3 Concluding Remarks

In this work the results of a comprehensive study of gallium arsenide doped with a transition metal (copper) by thermal diffusion are presented. The *recipe* for compensation has been shown, and verification of the deep levels created has been demonstrated for

various processing parameters. Several important parameters were measured for the first time such as the compensation curve, saturation of the on-state conductivity, and hole trapping time. Also, the physical location of copper in these wafers was measured using mass spectroscopy techniques. The goal of this work was to compensate the n-type gallium arsenide through the thermal diffusion of copper and characterize the resulting material to determine the electrical and physical properties. The results show that the processing parameters such as arsenic pressure in the ampoule, and annealing temperature are very important parameters in the development of uniform, compensated material. The physical characterization techniques employed here have shown that the diffusion of copper into gallium arsenide is a non-uniform process. Therefore, future work must involve improved processing techniques such as copper-doping during the growth of the ingot.

From this work it is possible to develop devices which rely on copper in gallium arsenide. The BOSS photoconductive switch is an example of a device which uses the optical and electronic properties of diffused copper for operation. The design of such a device involves the use of compensation, and IR-photoconductive properties. For example, in order to design a switch that operates on a sub-nanosecond time scale, the silicon-density in the material must be about $1x10^{16}$ cm^{-3}. This means that the diffusion temperature is about 560 °C, which corresponds to a Cu-density of about $2x10^{16}$ cm^{-3}. The on-state conductivity of this device will be about 1 $(\Omega cm)^{-1}$, and the turn-off time can be on the order of 140 ps provided there is a recombination channel of similar speed. If

higher on-state conductivity is required, then higher doping densities are required which sacrifices some of the turn-off speed (a few ns compared to 140 ps).

REFERENCES

1. S.M. Sze, Semiconductor Devices: Physics and Technology, Bell Telephone Laboratories, Inc., 1985.

2. K. H. Schoenbach, V. K. Lakdawala, R. Germer, and S. T. Ko, J. Appl. Phys., **63**, 2460, 1988.

3. M. S. Mazzola, K. H. Schoenbach, V. K. Lakdawala, and R. Germer, Appl. Phys. Lett., **54**, 742, 1989.

4. M. S. Mazzola, K. H. Schoenbach, V. K. Lakdawala, and S. T. Ko, Appl. Phys. Lett., **55**, 2102, 1989.

5. R. A. Roush, D. C. Stoudt, M. S. Mazzola, Appl. Phys. Lett., **62**, 2670, 1993.

6. Haisty, E. W. Mehal, and R. Stratton, J. Phys. Chem. Solids, **23**, 829, 1962.

7. Secondary Ion and Glow Discharge Mass Spectrometers are operated by Steve Schaur, and Andrew Souzis at Electronic Devices Laboratory (ETDL) at Ft. Monmouth, New Jersey.

8. R. P. Brinkmann, K. H. Schoenbach, M. S. Mazzola, R. A. Roush, and D. C. Stoudt, Proceedings of the SPIE Conference, Los Angeles California, 1993.

9. Markowich, C. A. Ringhofer, C. Schmeiser, Semiconductor Equations, Springer-Verlag: New York, (1990), pgs. 104-171.

10. R. A. Roush, M. S. Mazzola, and D. C. Stoudt, IEEE Transactions on Electron Devices, **40**, 1081, 1993.

11. Kullendorff, L. Jansson, and L. A. Ledebo, J. Appl. Phys., **54**, 3203, 1983.

12. M. Martin, J. P. Farges, G. Jacob, and J. P. Hallais, J. Appl. Phys, **51**, 2840.

13. Johnson, J. A. Kafalas, and R. W. Davies, J. Appl. Phys., **54**, 204, 1983.

14. R. N. Hall and J. Racette, J. Appl. Phys., **35**, 379, 1964.

15. Fuller, and H. M. Whelan, J. Phys. Chem. Solids, **6**, 173, 1958.

16. Zakharova, M. A. Krivov, E. V. Malisova, and E. A. Popova, Soviet Phys.-Semiconductors, **6**, 171, 1972.

17. Hutchinson, and R. K. Ball, J. Mat. Science, **17**, 406, 1982.

18. Furukawa, K. Kajiyama, and T. Aoki, Jap. J. Appl. Phys., **5**, 39, 1966.

19. Tin, C. K. Teh, and F. L. Weichman, J. Appl. Phys. **62**, 2329, 1987.

20. Tin, C. K. Teh, and F. L. Weichman, J. Appl. Phys. **63**, 355, 1988.

21. L. M. Thomas, and V. K. Lakdawala, J. Elect. Mat., **22**, 341, 1993.

22. Asom, Appl. Phys. Lett., **52**, 1472 1988.

23. Hurle, J. Phys. Chem. Solids, **40**, 627, 1979.

24. A. G. Milnes, "Impurity and Defect Levels (Experimental) in Gallium Arsenide," in Advances in Electronics and Electron Physics, vol. 61, edited by P. W. Hawkes, Acedemic Press: New York (1983), pgs. 63-159.

25. Nishizawa, H. Otsuka, S. Yamakoshi, and K. Ishida, Jap. J. Appl. Phys., **13**, 46, 1974.

26. Shih, J. W. Allen, and G. L. Pearson, J. Phys. Chem. Solids, **29**, 379, 1968.

27. Munoz, W. L. Snyder, and J. L. Moll, Appl. Phys. Lett. **16**, 262, 1970.

28. Potts, and G. L. Pearson, J. Appl. Phys. **37**, 2098, 1966.

29. Lee, R. Gronsky, and E. D. Bourret, J. Appl. Phys. **64**, 114, 1988.

30. Otsuka, K. Ishida, and J. Nishizawa, Jap. J. Appl. Phys. **8**, 632, 1969.

31. Braslau, J. B. Gunn, and J. L. Staples, Solid-State Elect. **10**, 381, 1967.

32. H. Holloway, and L. Yeh, Appl. Phys. Lett. **59**, 947, 1991.

33. Kuan, P. E. Batson, T. N. Jackson, H. Rupprecht, and E. L. Wilkie, J. Appl. Phys. **54**, 6952, 1983.

34. Ogawa, J. Appl. Phys. **51**, 406, 1980.

35. Yoder, Solid-State Elect. **23**, 117, 1980.

36. Brozel, J. B. Clegg, and R. C. Newman, J. Phys. D: Appl. Phys., **11**, 1331, 1978.

37. G. Spitzer and W. Aldred, J. Appl. Phys. **29**, 4999, 1968.

38. Chang, L. Esaki, and R. Tsu, Appl. Phys. Lett. **19**, 143, 1971.

39. Bourgoin, H. J. von Bardeleben, and D. Stievenard, J. Appl. Phys. **64**, R65, 1988.

40. van der Pauw, Philips Res. Repts. **13**, 1, 1958.

41. Fuller, K. B. Wolfstirn, and H. W. Allison, J. Appl. Phys. **38**, 2873, 1967.

42. D. C. Look, and S. Chaudhuri, Phys. Rev. Lett. **49**, 1728, 1982.

43. Hiesinger, Phys. Stat. Sol. (a) **33**, K39, 1976.

44. J. S. Blakemore, Semiconductor Statistics, Pergamon Press: New York (1962), pg. 139.

APPENDIX A

PASCAL CODE FOR COMPENSATION CURVE MODEL

```
{$M 65520, 0, 655360}
{$N+}
{$E+}
{$D+}
{$L+}

(*
(*      THIS PROGRAM COMPUTES THE CONDUCTIVITY FOR GaAs WITH SEVERAL
(*      AND/OR ACCEPTORS.  FERMI-DIRAC STATISTICS ARE USED TO CALCULATE
(*      THE FERMI-LEVEL FROM WHICH THE CONDUCTIVITY CAN BE FOUND.
(*      THE CONCUTIVTIY IS CALCULATED AS A FUNCTION OF THE DOPING DENSITY
(*      OF ANY OF THE LEVELS.
(*
(*
(*                              WRITTEN BY:    RANDY ROUSH (1995)
(*



Uses Crt, Functs;

Var n, p, CUA, CUB, EL2, Si, NA1, NA2, ND1, ND2, sigma, Fermi_Level : extended;
Var NC, EC, q, Partition, LHS1, LHS2, kT, diff : Extended;
Var RHS, LHS, Mun, Mup, ni, k, T, Ratio, EL5, ND3 : extended;
Var LHS3, LHS4, LHS5, EF, EFTest, increment : extended;
Var i : integer;
Var Data1,Data2 : Text;
Var OutFile1, Outfile2 : String;
Begin
(*
ClrScr;

Writeln('This program calculates the conductivity as a function of deep');
writeln('acceptor density for GaAs with two acceptor levels and two donor');
Writeln('levels.');
Writeln(' ');
Writeln(' ');
Writeln('Enter the energy (with respect to the valence band) for the first');
Write('acceptor level in eV:  ');
Readln(CUA);
Writeln(' ');
```

```
Write('Enter the energy for the second acceptor level in eV: ');
Readln(CUB);
Writeln(' ');
Write('Enter the ratio of the two acceptor densities (ie. first/second): ');
Readln(Partition);

ClrScr;

Writeln(' ');
Write('Enter the energy for the deep donor level in eV: ');
Readln(EL2);
Writeln(' ');
Writeln(' ');
Write('Enter the density of the shallow donor level in cm-3: ');
Readln(ND1);
Writeln(' ');
Write('Enter the density of the deep donor level in cm-3: ');
Readln(ND2);  *)
ClrScr;
Writeln(' ');
Writeln('Enter the name of the output file for total acceptor concentration');
Write('and conductivity: ');
Readln(OutFile1);
Assign(Data1,OutFile1);
Rewrite(Data1);
Writeln('Enter the name of the output file for free electron and hole');
Write('concentrations: ');
Readln(Outfile2);
Assign(Data2,Outfile2);
Rewrite(Data2);


(*                                    *)
(*       Begin Computations                    *)


CUA := 0.14;
CUB := 0.44;
Si := 1.4142;
EL2 := 0.59;
EL5 := 1.01;
ND1 := 5e16;
ND2 := 1e16;
ND3 := 0;



q := 1.602e-19;
k := 1.38062e-23;
NC := 5e17;
EC := 1.42;
T := 300;
ni := 2.6e6;
kT := k*T/q;
```

```
i:=0;


Mun := 4000;
Mup := 300;


NA1 := 2e14;
Partition := 0.2;

While NA1 < 2e17 Do

 Begin
 NA2 := NA1/Partition;
 EF := 0.01;
 increment := 0.01;

   While EF < EC Do
     Begin
     n := NC*exp((EF-EC)/kT);
     LHS1 := NA1/(1+4*exp((CUA-EF)/kT));
     LHS2 := NA2/(1+4*exp((CUB-EF)/kT));
     LHS3 := ND1/(1+2*exp((EF-Si)/kT));
     LHS4 := ND2/(1+2*exp((EF-EL2)/kT));
     LHS5 := ND3/(1+2*exp((EF-EL5)/kT));
     RHS := ni*ni;
     LHS := n*(LHS1+LHS2-LHS3-LHS4-LHS5) + n*n;


     If LHS < 0 then
       Begin
       EFTest := EF;
       EF := EF + increment/10;
       i:=1;
       end;


     Diff := RHS-LHS;

       If Diff < 0 then
         Begin
         i:=1;
         EFTest := EF;
         EF := EF - increment;
         increment := increment/10;
         end;


     Ratio := LHS/rhs;

     If Ratio > 0.9 then
        If Ratio < 1.1 then
        Begin
        Fermi_Level := EF;
```

```
            EF := 5;
            End;

        If EF - EFTest < 0.00001 Then
            Begin
            Fermi_Level := EF;
            EF := 5;
            end;

(*      Writeln(lhs1, Lhs2,lhs3); *)
        If i = 0 then EFTest := EF;
        If i = 0 then EF := EF + increment;

        i:=0;
        End;


    p:= ni*ni/n;
    Sigma := q *(Mun*n + Mup*p);
    Writeln(Sigma,n,p);
    Writeln(Data1,(NA1+NA2),Sigma);
    Writeln(Data2,Fermi_Level,n,p);
    NA1:=NA1*1.01;

End;
End.
```

APPENDIX B

PASCAL CODE FOR AUTOMATED HALL EFFECT MEASUREMENTS

```
Program Hall_Measurements_And_Calculations;

(*
(*
(*      THIS PROGRAM CONTROLS THE FOUR KEITHELY INSTRUMENTS USING GPIB, THE
(*      ELECTROMAGNET VIA LPT1 PORT, AND OMEGA THERMOMETER BY SERIAL PORT.
(*      THE PROGRAM PERFORMS HALL MEASUREMENTS OVER A WIDE TEMPERATURE
(*      RANGE (100-600 K) BY TAKING DATA EVERY 1 K. MOBILITY, CARRIER
(*      CONCENTRATION, CONDUCTIVITY, AND CARRIER TYPE ARE ALL STORED DURING
(*      THE EXPERIMENT.
(*
(*
(*              WRITTEN BY:   RANDY ROUSH   (1994)


{$V-}
{$M 65520, 0, 655360}
{$N+}
{$E+}
{$D+}
{$L+}
{$R+}  (* Range checking on *)

Uses dos, tpdecl, Tempread, crt, graph; (* HallGrap; *)

Var t, j, ii, jj, BRD0, M7001, M220, M196, M485, NumSets, SetTime1:Integer;
Var Resistivity, CMD1, DATA1, InVal, Field, mode, TTemp:String;
Var V, I, HallVolt:Array[1..8] of Real;
Var VRead, IRead, PosVoltage, NegVoltage, PosCurrent, NegCurrent:Real;
Var PosHallVolt, NegHallVolt, Voltage, Current, Temp, Temp1, Temp2, d:Real;
Var TempInterval, MaxTemp, DeltaTemp, MaxDeltaTemp, MinHotTemp, MaxColdTemp:Real;
Var Rho, Temperature, Mu:Array[1..1000] of Extended;
Var DNA:Extended;
Var CMD,Data:cbuf;
Var Name,FILENAME, single:String;
Var File1:Text;
Var B:Real;
Const q = 1.602e-19;

Const Res:Array[1..4] of String = ('1243','4312','3241','4132');
```

```
Const Hall:Array[1..2] of String = ('4231','3142');

Procedure Input_Info;
var dummy:string;
var junk:real;
var C:integer;
Begin
   ClrScr;
   Writeln;
   Writeln;
   Writeln;
   Writeln;
   Writeln;
   Writeln('          TEMPERATURE DEPENDENT HALL MEASUREMENT          ');
   writeln;
   Writeln;
   Writeln;
   InVal := '1.5e-3';
   Mode := 'lo';
   NumSets := 5;
   SetTime1 :=2000;
   TTemp := 'z';
   MinHotTemp := 300;
   MaxColdTemp:= 520;
   TempInterval := 1;
   MaxDeltaTemp := 3;
   d := 0.07;
   B := 1450;
   FILENAME := 'c:\hall\HALL.DAT';
   single := 'n';
   Writeln('              PRESENT CONFIGURATION     ');
   WRITEln;
   writeln;
   writeln('Current = ',inval:1,'    Resistivity Mode, ', mode, '   Settling Time = ',settime1/1000:1:1 ,'
seconds');
   writeln;
   writeln('Sample Thickness = ',d:1:3,' cm.        Magnetic Flux Density = ',B:1:1,' gauss');
   Writeln;
   writeln;
   writeln('Would you like to change any of these? (y or n)');
   readln(dummy);
   If dummy = 'y' then
     begin
       writeln('Input the current (ex. 1e-3 for 1 mA)...   (1.9 mA max)');
       readln(InVal);
       repeat
         val(InVal,junk,C);
         If junk > 1.98e-3 then
         Begin
           writeln('ERROR!! Current value cannot be used. Input new current value less than 1.99
mA.');
           readln(InVal);
         end;
       until junk < 2e-3;
```

```
        writeln;
        writeln('Input the resistivity mode ("hi" or "lo")...');
        readln(mode);
        writeln;
        writeln('Input the settling time in seconds...');
        readln(settime1);
        settime1 := settime1 *1000;
        writeln;
        writeln('Input the Sample Thickness in cm...');
        readln(d);
        writeln;
        writeln('Input the magnetic flux density in gauss...');
        readln(B);
        writeln;
    end;
    Writeln;
    Writeln('Will this be a single hall measurement at one temperature? (y or n)');
    readln(single);
    If single = 'n' then
    begin
      writeln('Will the sample be initially heated or cooled? (c - cooled, h - heated)');
      readln(TTemp);
    end;
    Clrscr;
    Writeln('Input the filename... (ex. C:\HALL\HALL.DAT)');
    readln(filename);

End;


Procedure CloseCrossPoints(CD:cbuf);

Begin
     If Resistivity = 'Off' then
     Begin
        Data[11] := Hall[j,1];
        Data[17] := Hall[j,2];
        Data[23] := Hall[j,3];
        Data[29] := Hall[j,4];
     End;

     If Resistivity = 'On' then
     Begin
        Data[11] := Res[j,1];
        Data[17] := Res[j,2];
        Data[23] := Res[j,3];
        Data[29] := Res[j,4];
     End;

     Data[2] := 'C';
     Data[3] := 'L';
     Data[4] := 'O';
     Data[5] := 'S';
```

```
        ibwrt(M7001, Data, length(Data1));
        End;

Procedure CrossPointsOpen(CD:cbuf);

Begin


        Data[2] := 'O';
        Data[3] := 'P';
        Data[4] := 'E';
        Data[5] := 'N';

        ibwrt(M7001, Data, length(Data1));

        End;

Procedure Disable220Current;

        (*  Turn-Off the 220 Source    *)
        Begin

        CMD[1] := 'F';
        CMD[2] := '0';
        CMD[3] := 'X';
        ibwrt(M220, CMD, 3);

        End;

Procedure OpenMostCrossPoints;

        Begin

        (* Call this procedure to make sure all crosspoints on the 7001  *)
        (* are opened. The user can abort from a series of measurements.*)
        (* This may occur during a point when some of the crosspoints are*)
        (* closed. It is a good thing to call this procedure before     *)
        (* beginning a series of measurements.                          *)

        CMD1 := ':OPEN (@1!1!1:1!4!4)';
        For t := 1 to Length(CMD1) Do
        Begin
          CMD[t] := CMD1[t];
        End;
        IBWRT(M7001, CMD, Length(CMD1));

        End;

Procedure Send_Error_Message;

Begin
        Writeln('The voltage at the Hall Card has exceeded the limit');
```

```
End;


Function Blanks_Away(H:String):String;

Var A :String;
Var AA:Real;
Var C : integer;

Begin

   A := H;
   t := 1;
   While  (A<>'') and (A[t] <> 'E') do  t := t + 1;
   A := Copy(A,4,t-1);

   Val(A,AA,C);
   If AA > 0.095 Then A:= Copy(A,4,t); (*  Necessary for 1e-10 and less.  *)

   Blanks_Away := A;

End;


Procedure Get_Pos_Data_Set;

Var SPACE,VReadingPoint, IReadingPoint:String;
Var Voltage, Current:Real;
Var C,ii:Integer;

Begin

   Voltage := 0;
   Current := 0;

   For ii := 1 to NumSets Do

   Begin

      IBRD(M196, VReadingPoint, 100);
                                  (*  Gets rid of leading and *)
      VReadingPoint := Blanks_Away(VReadingPoint); (*  trailing spaces       *)

      VAL(VReadingPoint,VRead,C);
      If ABS(VRead) > 8 Then (* Disable Source Current  *)
        Begin
           CMD[1] := 'F';
           CMD[2] := '0';
           CMD[3] := 'X';
           IBWRT(M220, CMD,3);
           OpenMostCrossPoints;
           Send_Error_Message;
           Halt(1);
        End;
```

```
      (*  Read Current, Display, and save to File  *)

      IBRD(M485, IReadingPoint,100);

                                  (* Gets Rid of leading and *)
      IReadingPoint := Blanks_Away(IReadingPoint); (* trailing spaces      *)

      VAL(IReadingPoint, IRead, C);

      Voltage := Voltage + VRead;  (* Get average of NumSets of  *)
      Current := Current + IRead;  (* data                       *)

   End;

   PosVoltage := Voltage/NumSets;
   PosCurrent := Current/NumSets;

End;


Procedure Get_Data_Set;

Var VReadingPoint, IReadingPoint:String;
Var C, ii:Integer;

Begin

   Voltage := 0;
   Current := 0;
   NegHallVolt := 0;

   For ii := 1 to NumSets Do

   Begin

     IBRD(M196, VReadingPoint, 100);

                                  (* Gets rid of leading and *)
     VReadingPoint := Blanks_Away(VReadingPoint);  (* trailing spaces      *)


     VAL(VReadingPoint,VRead,C);
     If ABS(VRead) > 8 Then (* Disable Source Current  *)
       Begin
          CMD[1] := 'F';
          CMD[2] := '0';
          CMD[3] := 'X';
          IBWRT(M220, CMD,3);
          OpenMostCrossPoints;
          Send_Error_Message;
          Halt(1);
          End;

     (*  Read Current, Display, and save to File  *)
```

```
      IBRD(M485, IReadingPoint, 100);
                              (* Gets Rid of leading and *)
      IReadingPoint := Blanks_Away(IReadingPoint); (* trailing spaces      *)

      VAL(IReadingPoint, IRead, C);

      Voltage := Voltage + VRead;
      Current := Current + IRead;

      End;

      NegVoltage := Voltage/NumSets; (* Get average of NumSets of  *)
      NegCurrent := Current/NumSets; (* data                       *)

      V[j] := (PosVoltage - NegVoltage)/2;
      I[j] := (PosCurrent - NegCurrent)/2;


   If Resistivity = 'Off' Then
   Begin
      NegVoltage := -NegVoltage;
      If field = 'Pos' then PosHallVolt := (PosVoltage+NegVoltage)/2;
      If field = 'Neg' then NegHallVolt := (PosVoltage+NegVoltage)/2;
      HallVolt[j] := PosHallVolt - NegHallVolt;

   End;

End;



Procedure InitNationalController;

Var Addr220, Addr196, Addr7001, Addr485, BRD0:Integer;
Var NA:nbuf;

Begin
      (*  Define instrument primary addresses    *)

      Addr220  := 12;
      Addr196  :=  7;
      Addr7001 :=  8;
      Addr485  := 22;


      NA := 'GPIB0  ';
        BRD0 := IBFIND (NA);   (* Find board Descriptor  *)
      NA := 'DEV1   ';
        M220 := IBFIND (NA);   (* Find 220 Descriptor    *)
      NA := 'DEV2   ';
        M196 := IBFIND (NA);   (* Find 196 Descriptor    *)
      NA := 'DEV3   ';
        M7001 := IBFIND (NA);  (* Find 7001 Descriptor   *)
      NA := 'DEV4   ';
```

```
    M485 := IBFIND (NA);   (* Find 485 Descriptor    *)

  IBPAD(M220, Addr220);   (* Set 220 Primary Address *)
  IBPAD(M196, Addr196);   (* Set 196 Primary Address *)
  IBPAD(M7001, Addr7001); (* Set 7001 Primary Address*)
  IBPAD(M485, Addr485);   (* Set 485 Primary Address *)

  IBTMO(BRD0, 13);        (* Set Timeout to 10 Sec. *)

  End;


Procedure Zero_SpollByte;

Var x, msg:String;
Var SpollByte, t:Integer;
Begin
    Repeat


 (*     Repeat IBRSP(M220, SpollByte) Until SpollByte = 0;*)

      CMD[1] := 'I';
      For t := 1 to Length(InVal) Do
      Begin
        CMD[t+1] := InVal[t];
      End;

      CMD[Length(InVal)+2] := 'X';

      CloseCrossPoints(Data);
      ibwrt(M220, CMD, Length(InVal)+2);    (* Program the 220 Current   *)
      CMD[1] := 'F';
      CMD[2] := '1';
      CMD[3] := 'X';
      ibwrt(M220, CMD, 3);
      Delay(2000);       (* Allow the 220 to execute the current *)
                 (* command. That way if an error occurs*)
                 (* the SPOLL byte read will be after the*)
                 (* error which will give an actual error*)
                 (* code. This is what we want.        *)
      IBRSP(M220, SpollByte);
      If (SpollByte and $2) <> 0 then
      Begin
        msg := 'The 220 Current was not Programmed Properly!';
        MSG := msg + ' Please enter a proper current value.';

        Writeln(MSG);
        ReadLn(InVal);
      End;

    Disable220Current;
    Writeln('Opening Cross Points');
    OpenMostCrossPoints;
```

```
        Until (SpollByte and $2) = 0;
End;



Procedure MeasVoltInstrInit;

Var SpollByte, Variable:Integer;
Var HiResistivity:Boolean;

Begin


        Variable := 1;
        CMD[1] := 'D';
        CMD[2] := 'C';
        CMD[3] := 'L';

        IBSRE(brd0, Variable);    (* Send Remote Enable   *)
        IBCMD(brd0, CMD, 3);        (* Send Device Clear    *)

(* Initialize 7001  *)

Writeln('Initializing the 7001');
        CMD1 := ':OPEN (@1!1!1:1!4!4)';
        For t := 1 to Length(CMD1) Do
        Begin
           CMD[t] := CMD1[t];
        End;

        ibwrt(M7001, CMD, Length(CMD1));

        IF Mode = 'hi' then
         Begin
          CMD1 := ':CLOS (@1!4!5)';      (* Select High Res. Mode  *)
          For t := 1 to Length(CMD1) Do
           Begin
              CMD[t] := CMD1[t];
           End;
         End;
        IF Mode = 'lo' then
         Begin
           CMD1 := ':OPEN (@1!4!5)';  (* Select Low Res. Mode   *)
           For t := 1 to Length(CMD1) Do
           Begin
              CMD[t] := CMD1[t];
           End;
         End;

        Writeln('Selecting "',Mode,'" Resistivity Mode...');
        Delay(500);
        ibwrt(M7001, CMD, 14);  (* Program Card Resistivity Setup *)
        Delay(500);
```

```
(* Initialize 485 *)

        CMD[1] := 'R';
        CMD[2] := '1';
        CMD[3] := 'X';              (* Select 2 nA Range   *)
        ibwrt(M485, CMD, 3);
Writeln('Selecting 2 nA Range');
        Delay(500);

        CMD[1] := 'C';              (* Enable Zero Check   *)
        CMD[2] := '1';
        CMD[3] := 'X';
        ibwrt(M485, CMD, 3);
Writeln('Enable Zero Check');
        Delay(500);

        CMD[1] := 'Z';
        CMD[2] := '1';
        CMD[3] := 'X';              (* Enable 485 Rel Mode *)
        ibwrt(M485, CMD, 3);
Writeln('Enable 485 Rel Mode');
        Delay(500);

        CMD[1] := 'C';
        CMD[2] := '0';
        CMD[3] := 'X';              (* Disable 485 Zero Check *)
        ibwrt(M485, CMD, 3);
Writeln('Disable 485 Zero Check');
        Delay(500);

        CMD[1] := 'R';
        CMD[2] := '0';
        CMD[3] := 'G';
        CMD[4] := '0';
        CMD[5] := 'X';
        CMD[6] := 'Y';
        CMD[7] := 'X';              (* Enable 485 Auto Range *)
        ibwrt(M485, CMD, 7);
Writeln('Enable 485 Auto Range');
        Delay(500);


(* Initialize 196 *)

Writeln('Configure 196 DMM for Auto, DCV, Rate, No Prefix, CR LF');
        CMD[1] := 'R';   (*      Configure 196 DMM       *)
        CMD[2] := '0';
        CMD[3] := 'F';
        CMD[4] := '0';
        CMD[5] := 'S';
        CMD[6] := '3';
        CMD[7] := 'G';
        CMD[8] := '0';
        CMD[9] := 'Y';
```

```
        CMD[10] := '0';
        CMD[11] := 'X';

        ibwrt(M196, CMD, 11);       (* Auto, DCV, Rate, No Prefix, CR LF *)
                        (* terminator                    *)
        Delay(500);

(*  Initialize 220  *)

Writeln('Initialize the 220 source');

        CMD[1] := 'V';
        CMD[2] := '1';
        CMD[3] := '0';
        CMD[4] := 'X';          (*   10V Compliance              *)
        ibwrt(M220, CMD, 4);

        Zero_SpollByte;

(*  Zeroing SPOLL byte is necessary after the 220 powers up *)


      End;


Procedure NegativeCurrentOutput;

Begin
        InVal := '-' + InVal;

        CMD[1] := 'I';
        For t := 1 to Length(InVal) Do
           Begin
           CMD[t+1] := InVal[t];
           End;
        CMD[Length(InVal)+2] := 'X';

        ibwrt(M220, CMD, Length(InVal)+2); (* Configure for the negative current.  *)

        CMD[1] := 'F';
        CMD[2] := '1';
        CMD[3] := 'X';
        ibwrt(M220, CMD, 3);
        InVal := Copy(InVal,2,Length(InVal));
        End;


Procedure PositiveCurrentOutput;

Begin
        (* The assumption is made that the current value is a valid   *)
        (* value that the 220 can accept.                    *)

        CMD[1] := 'I';
```

```
        For t := 1 to Length(InVal) Do
          Begin
          CMD[t+1] := InVal[t];
          End;
        CMD[Length(InVal)+2] := 'X';

        ibwrt(M220, CMD, length(InVal)+2);      (* Program the 220 current with *)

        CMD[1] := 'F';
        CMD[2] := '1';
        CMD[3] := 'X';          (* Enable the current output    *)
        ibwrt(M220, CMD, 3);

        End;


Procedure Turn_On_Magnet;

Begin
        Field := 'Pos';
        Port[$378] := 1;
        end;


Procedure Turn_Off_Magnet;

Begin
        Port[$378] := 0;
        end;


Procedure Reverse_Polarity;

Begin
        Port[$378] := 2;
        end;


Procedure Turn_On_Reverse_Magnet;

Begin
        Field := 'Neg';
        Port[$378] := 3;
        end;

Function F_Factor:Real;
var a,b,c,d,x,F:Real;
Begin
    a:=1.0816;
    b:=0.9189;
    c:=11.0816;
    d:=0.2065;
    x:=(V[1]/I[1])/(V[3]/I[3]);
    If x < 1 then x := 1/x;
```

```
   F:=((a-d)/(1+exp(b*ln(x/c)))) + d;
   F_Factor := F;
   writeln('                    F_Factor is, ',F:0:5);
End;


Procedure Calculate_Resistivity;

Var IAvg1, IAvg2, IAvg, VAvg, VAvg1, Vavg2, Rho1, Rho2:Extended;


Begin

      IAvg1 := (I[1]+I[2])/2;
      VAvg1 := (V[1]+V[2])/2;
      IAvg2 := (I[3]+I[4])/2;
      VAvg2 := (V[3]+V[4])/2;
      IAvg := (IAvg1+IAvg2)/2;
      VAvg := (VAvg1+VAvg2)/2;


      Rho[jj] := F_Factor * abs((pi*d/ln(2))*VAvg/IAvg);

      End;


Procedure Calculate_Mobility;

Var DeltaV,IAvg:Real;
Var RH:Extended;
Begin

      DeltaV := (HallVolt[1]-HallVolt[2])/2;
      IAvg := (I[1]+I[2])/2;
      RH := 1e8*d*DeltaV/(2*B*IAvg);

      Mu[jj] := RH/Rho[jj];

      End;



Procedure Check_Delta_Temp;

Var NewTime:String;
Var C:integer;
Begin

      If DeltaTemp >= MaxDeltaTemp Then
      Begin
         rho[jj]:=0;
         mu[jj] :=0;
      End;
```

```
End;


Procedure Temperature_Decision;
var ttt:integer;
Begin
      Repeat
      ttt:=0;
      Temp := Read_In_Temperature;
      ttt:= ttt+1;
      Until ABS(Temp1 - Temp) >= TempInterval;
End;

Procedure Set_Up_Data_File;
Begin
 Name := FILENAME;
 Assign(File1,Name);
 Rewrite(File1);
End;


Procedure Store_Data;
var carrier_type:string;
Begin

If mu[jj]<0 then carrier_type := 'n-type' else carrier_type := 'p-type';
mu[jj] := abs(mu[jj]);
writeln(File1,Rho[jj]:0:9,'  ',Mu[jj]:0:7,'  ',Temperature[jj]:0:1,'  ',carrier_type);

End;




(* ***************  MAIN PROGRAM  ***************** *)



(*  Var n:Array[1..4] of String; *)
Var C:Integer;


BEGIN

Port[$378] := 0;    (*  Initialize the LPT1 port with zeros  *)
Resistivity := 'DontCare';
DATA1 := ':CLOS (@1!1!2,1!2!1,1!4!3,1!3!4)';
For t := 1 to Length(Data1) Do
Begin
   DATA[t] := DATA1[t]
End;
```

```
Input_Info;

(* Set_Up_Graph; *)

InitNationalController;
MeasVoltInstrInit;          (* Initialize Instruments          *)
clrscr;

writeln('The instruments have been successfully initialized.');
writeln(' ');
writeln('Press any key to begin experiment...  (Ctrl-Break to exit)');

Temp1 := 0;

   Temp := Read_In_Temperature;
   Temp := Read_In_Temperature;
   Repeat
    until keypressed;
    Temp2:= Read_In_Temperature;
    Temp := Read_In_Temperature;
    ClrScr;

Set_Up_Data_File;

jj := 1;

If Single = 'y' then
Begin

  Temperature_Decision;

      For j := 1 to 4 Do
      Begin
         Resistivity := 'On';

         CloseCrossPoints(Data);
         PositiveCurrentOutput;
          Delay(SetTime1);
          Get_Pos_Data_Set;
          Disable220Current;
         delay(100);
         NegativeCurrentOutput;
          Delay(SetTime1);
          Get_Data_Set;
         Disable220Current;
         CrossPointsOpen(Data);

                (*  The Current, Res_Data[j-3], is, I[j/4]);  *)
                (*  The Voltage, Res_Data[j-2], is, V[j/4]);  *)
      End;

      Calculate_Resistivity;

      For j := 1 to 2 Do
```

```
        Begin
        Resistivity := 'Off';

           CloseCrossPoints(Data);
           PositiveCurrentOutput;
            Turn_On_Magnet;
            Delay(SetTime1);
            Get_Pos_Data_Set;
            Disable220Current;
            delay(100);
           NegativeCurrentOutput;
            Delay(SetTime1);
            Get_Data_Set;
            Disable220Current;
            Turn_Off_Magnet;
            Reverse_Polarity;
           Turn_On_Reverse_Magnet;
           delay(100);
           PositiveCurrentOutput;
            Delay(SetTime1);
            Get_Pos_Data_Set;
            Disable220Current;
           NegativeCurrentOutput;
            Delay(SetTime1);
            Get_Data_Set;
            Disable220Current;
           Turn_Off_Magnet;
           CrossPointsOpen(Data);

        End;

        Temp1 := Temp;
        Temp := Read_In_Temperature;
        Temp2 := Temp;

        DeltaTemp := Temp1 - Temp2;  (* Temp difference for before and *)
                              (* after data sets taken.        *)

        Temperature[jj] := (Temp1 + Temp2)/2;

        Calculate_Mobility;

        writeln(Rho[jj]:0:7,'  ',abs(Mu[jj]):0:3,'  ',Temperature[jj]:0:1);

        Check_Delta_Temp;

        Store_Data;

        jj := jj + 1;


    End;
```

```
If TTemp = 'c' Then While Temp <= MaxColdTemp Do
(* If TTemp = 'h' Then While Temp >= MinHotTemp Do *)

Begin

  Temperature_Decision;

      For j := 1 to 4 Do
      Begin
         Resistivity := 'On';

         CloseCrossPoints(Data);
         PositiveCurrentOutput;
          Delay(SetTime1);
          Get_Pos_Data_Set;
          Disable220Current;
         delay(100);
         NegativeCurrentOutput;
          Delay(SetTime1);
          Get_Data_Set;
         Disable220Current;
         CrossPointsOpen(Data);

                (*  The Current, Res_Data[j-3], is, I[j/4]);  *)
                (*  The Voltage, Res_Data[j-2], is, V[j/4]);  *)
      End;

      Calculate_Resistivity;

      For j := 1 to 2 Do
      Begin
      Resistivity := 'Off';

         CloseCrossPoints(Data);
         PositiveCurrentOutput;
          Turn_On_Magnet;
          Delay(SetTime1);
          Get_Pos_Data_Set;
          Disable220Current;
          delay(100);
         NegativeCurrentOutput;
          Delay(SetTime1);
          Get_Data_Set;
          Disable220Current;
          Turn_Off_Magnet;
          Reverse_Polarity;
         Turn_On_Reverse_Magnet;
         delay(100);
         PositiveCurrentOutput;
          Delay(SetTime1);
          Get_Pos_Data_Set;
          Disable220Current;
         NegativeCurrentOutput;
```

```
        Delay(SetTime1);
        Get_Data_Set;
        Disable220Current;
      Turn_Off_Magnet;
      CrossPointsOpen(Data);

    End;

    Temp1 := Temp;
    Temp := Read_In_Temperature;
    Temp2 := Temp;

    DeltaTemp := Temp1 - Temp2;  (* Temp difference for before and *)
                        (* after data sets taken.        *)

    Temperature[jj] := (Temp1 + Temp2)/2;

    Calculate_Mobility;

    writeln(Rho[jj]:0:7, '  ', abs(Mu[jj]):0:5,'  ',Temperature[jj]:0:1);

    Check_Delta_Temp;

    Store_Data;

    jj := jj + 1;


End;

jj := jj-1;

OpenMostCrossPoints;

Close(File1);


End.
```